Article

Cell

Vaccine Mediated Protection Against Zika Virus-Induced Congenital Disease

Graphical Abstract

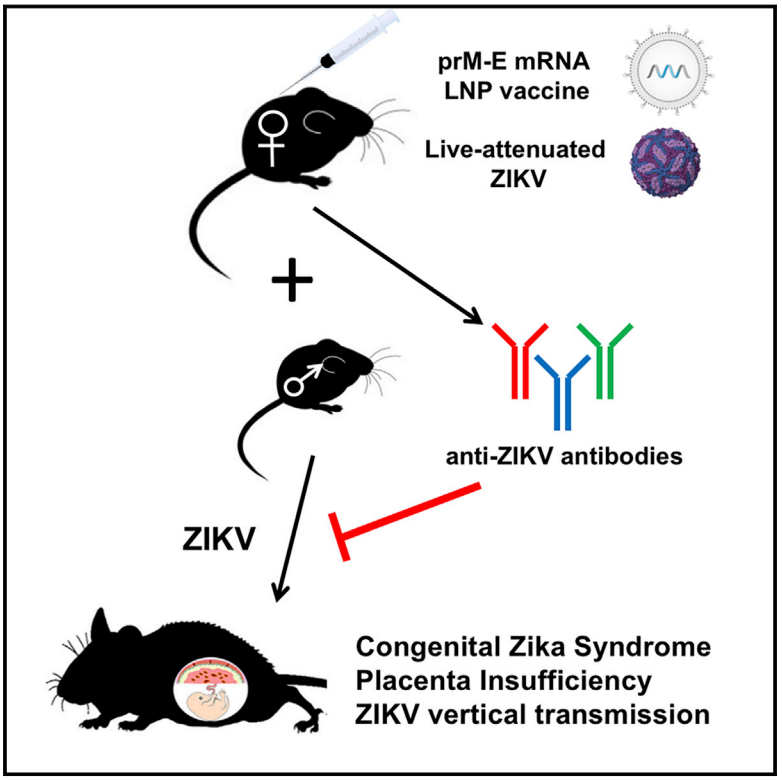

Highlights

- Modified mRNA and live attenuated ZIKV vaccines protect during pregnancy in mice
- High titers of neutralizing antibodies are achieved by both vaccine platforms
- Vaccines block ZIKV transmission to the fetus in most animals
- Damage to the placenta and fetus is prevented

Authors

Justin M. Richner, Brett W. Jagger, Chao Shan, ..., Theodore C. Pierson, Pei-Yong Shi, Michael S. Diamond

Correspondence

piersontc@niaid.nih.gov (T.C.P.), peshi@utmb.edu (P.-Y.S.), diamond@wusm.wustl.edu (M.S.D.)

In Brief

Immunization of pregnant animals with Zika virus vaccines protects the fetuses against vertical transmission of the virus, placental disease, and fetal demise.

Richner et al., 2017, Cell *170*, 273–283
July 13, 2017
http://dx.doi.org/10.1016/j.cell.2017.06.040

CellPress

Article

Cell

Vaccine Mediated Protection Against Zika Virus-Induced Congenital Disease

Justin M. Richner,[1,18,19] Brett W. Jagger,[1,18] Chao Shan,[2,18] Camila R. Fontes,[2,18] Kimberly A. Dowd,[3,18] Bin Cao,[4] Sunny Himansu,[5] Elizabeth A. Caine,[1] Bruno T.D. Nunes,[2,6] Daniele B.A. Medeiros,[2,6] Antonio E. Muruato,[2,7] Bryant M. Foreman,[3] Huanle Luo,[7] Tian Wang,[8,11] Alan D. Barrett,[7,11] Scott C. Weaver,[8,10,11] Pedro F.C. Vasconcelos,[6,15] Shannan L. Rossi,[7,10] Giuseppe Ciaramella,[5] Indira U. Mysorekar,[4,12] Theodore C. Pierson,[3,*] Pei-Yong Shi,[2,9,10,16,17,*] and Michael S. Diamond[1,12,13,14,20,*]

[1]Department of Medicine, Washington University School of Medicine, St. Louis, MO, USA
[2]Department of Biochemistry & Molecular Biology, University of Texas Medical Branch, Galveston, TX, USA
[3]Viral Pathogenesis Section, Laboratory of Viral Diseases, National Institutes of Health, Bethesda, MD USA
[4]Department of Obstetrics and Gynecology, Washington University School of Medicine, St. Louis, MO, USA
[5]Valera LLC, a Moderna Venture, 500 Technology Square, Cambridge, MA, USA
[6]Department of Arbovirology and Hemorrhagic Fevers, Evandro Chagas Institute, Ministry of Health, Ananindeua, Pará State, Brazil
[7]Department of Pathology, University of Texas Medical Branch, Galveston, TX, USA
[8]Department of Microbiology and Immunology, University of Texas Medical Branch, Galveston, TX, USA
[9]Institute for Translational Science, University of Texas Medical Branch, Galveston, TX, USA
[10]Institute for Human infections and Immunity, University of Texas Medical Branch, Galveston, TX, USA
[11]Sealy Center for Vaccine Development, University of Texas Medical Branch, Galveston, TX, USA
[12]Department of Pathology and Immunology, Washington University School of Medicine, St. Louis, MO, USA
[13]Department of Molecular Microbiology, Washington University School of Medicine, St. Louis, MO, USA
[14]The Andrew M. and Jane M. Bursky Center for Human Immunology and Immunotherapy Programs, Washington University School of Medicine, St. Louis, MO, USA
[15]Department of Pathology, Pará State University, Belém, Brazil
[16]Department of Pharmacology & Toxicology, University of Texas Medical Branch, Galveston, TX, USA
[17]Sealy Center for Structural Biology & Molecular Biophysics, University of Texas Medical Branch, Galveston, TX, USA
[18]These authors contributed equally
[19]Present address: IIT Research Institute, Chicago, IL, USA
[20]Lead Contact: Michael S. Diamond
*Correspondence: piersontc@niaid.nih.gov (T.C.P.), peshi@utmb.edu (P.-Y.S.), diamond@wusm.wustl.edu (M.S.D.)
http://dx.doi.org/10.1016/j.cell.2017.06.040

SUMMARY

The emergence of Zika virus (ZIKV) and its association with congenital malformations has prompted the rapid development of vaccines. Although efficacy with multiple viral vaccine platforms has been established in animals, no study has addressed protection during pregnancy. We tested in mice two vaccine platforms, a lipid nanoparticle-encapsulated modified mRNA vaccine encoding ZIKV prM and E genes and a live-attenuated ZIKV strain encoding an NS1 protein without glycosylation, for their ability to protect against transmission to the fetus. Vaccinated dams challenged with a heterologous ZIKV strain at embryo day 6 (E6) and evaluated at E13 showed markedly diminished levels of viral RNA in maternal, placental, and fetal tissues, which resulted in protection against placental damage and fetal demise. As modified mRNA and live-attenuated vaccine platforms can restrict in utero transmission of ZIKV in mice, their further development in humans to prevent congenital ZIKV syndrome is warranted.

INTRODUCTION

Zika virus (ZIKV) originally was identified in 1947 from a sentinel Rhesus macaque in the tree canopy of the Zika Forest of Uganda (Dick, 1952). In the past, ZIKV circulated between *Aedes* species mosquitoes and non-human primates, and intermittently caused human infections in restricted parts of Africa and Asia. Prior to 2010, ZIKV infection was described as a febrile illness associated with headache, rash, conjunctivitis, and muscle pain, and this mild clinical syndrome occurred in only about 20% of exposed individuals. More recently, and especially in the context of its spread to Oceania and the Americas, ZIKV infection has resulted in more severe clinical consequences (Faria et al., 2016; Lazear and Diamond, 2016). Particularly, maternal infection during pregnancy has been associated with placental insufficiency and numerous congenital malformations in the fetus including microcephaly and fetal demise (Brasil et al., 2016; Rasmussen et al., 2016). In addition, in a small subset of adults, ZIKV infection is linked to Guillain-Barré syndrome (GBS), an autoimmune polyneuropathy that can result in transient or sustained paralysis (Cao-Lormeau et al., 2016; Oehler et al., 2014). Sexual transmission of ZIKV also has been described, with persistence of infectious ZIKV or ZIKV RNA in semen, sperm, and vaginal secretions for up to 6 months following infection (Mansuy et al., 2016; Murray et al., 2017).

ZIKV is a member of the Flavivirus genus and *Flaviviridae* family of positive-polarity, enveloped RNA viruses (Pierson and Diamond, 2013). Translation of the infectious ~11 kilobase viral RNA in the cytoplasm produces a polyprotein that is cleaved into three structural proteins (capsid [C], pre-membrane/membrane [prM/M], and envelope [E]) and seven non-structural proteins (NS1, NS2A, NS2B, NS3, NS4A, NS4B, and NS5), which together coordinate replication, assembly of nascent virions, and immune evasion of the host. ZIKV buds into the endoplasmic reticulum lumen as an immature virion composed of icosahedrally arranged prM-E heterotrimers (Prasad et al., 2017). The acidic environment of the Golgi network triggers conformational changes in the virion that result in exposure of a furin protease cleavage site within prM. Cleavage of prM and eventual release of the pr peptide in the extracellular space produces mature, infectious virions that display 90 antiparallel E homodimers on their surface. The ZIKV E protein is the primary target of neutralizing antibodies (Heinz and Stiasny, 2017). Although ZIKV strains are classified into two genetic lineages (African and Asian/American) their divergence does not impact antibody neutralization significantly and thus, ZIKV is classified as a single serotype (Dowd et al., 2016a). ZIKV is related genetically to several pathogens that cause disease globally including dengue (DENV), West Nile (WNV), Japanese encephalitis (JEV), yellow fever (YFV), and tick-borne encephalitis (TBEV) viruses.

In a rapid response to the recent ZIKV epidemic, several groups have developed vaccine candidates based on subunit (prM-E or M-E DNA plasmid, adenovirus-vectored, or modified mRNA) or chemically inactivated whole-viral-particle approaches, all of which have elicited neutralizing antibodies that protect against ZIKV challenge in non-pregnant mice and non-human primates (Abbink et al., 2016; Dowd et al., 2016b; Larocca et al., 2016; Muthumani et al., 2016; Pardi and Weissman, 2017; Richner et al., 2017). While several of these vaccine candidates have advanced to phase 1 clinical trials in humans (Durbin, 2016), no study has established vaccine protection in the context of pregnancy.

Here, we evaluated a lipid-encapsulated (LNP) modified mRNA prM-E subunit vaccine (Richner et al., 2017) and a newly engineered live-attenuated ZIKV vaccine (ZIKV-NS1-LAV) encoding mutations in the NS1 gene that abolished both N-linked glycosylation sites for their ability to protect pregnant mice and their developing fetuses from ZIKV infection. Vaccination of wild-type (WT) female C57BL/6 mice with a two-dose regimen of the prM-E mRNA vaccine or a single dose of ZIKV-NS1-LAV induced high-titers of neutralizing antibodies. Immunized female mice were mated to WT male sires and then infected at embryo day 6 (E6) with a pathogenic heterologous African ZIKV strain. Whereas placebo-immunized mice developed high titers of ZIKV in the maternal tissues, placenta, and fetal brain, those vaccinated with the prM-E mRNA or ZIKV-NS1-LAV showed markedly diminished levels of virus in these tissues, with the majority of fetuses showing no evidence of infection.

RESULTS

Activity of a prM-E mRNA LNP Vaccine in Pregnancy

In recent studies, two groups showed that intramuscular or intradermal immunization of LNP-encapsulated modified mRNA vaccines encoding the prM-E genes of Asian-American ZIKV isolates protected non-pregnant adult mice or non-human primates against ZIKV viremia, tissue viral burden, or lethality in different challenge models (Pardi et al., 2017; Richner et al., 2017). As none of the existing ZIKV vaccine platforms (mRNA LNP, DNA plasmid, viral-vectored, or chemically inactivated virions) has been evaluated for protection of fetuses during pregnancy, we designed a trial to test this in mice. Eight-week-old WT immunocompetent C57BL/6 female mice were divided into two groups, with each receiving an intramuscular inoculation of 10 μg of prM-E mRNA containing a signal sequence from human IgE or non-translating mRNA LNPs. The two groups of female mice were boosted with the same dose of LNP vaccine at 28 days after immunization, bled at day 49 for serological analysis (see below), and then mated with 12-week-old WT C57BL/6 male mice at approximately day 56 and monitored for vaginal plugs, an indication of insemination (Figure 1A). To facilitate ZIKV replication in peripheral tissues and spread to the maternal decidua and placenta (Miner et al., 2016), we passively transferred 2 mg of a blocking anti-Ifnar1 antibody 1 day prior (embryo day 5 [E5]) to infection at E6 with 10^5 focus-forming units (FFU) of a heterologous mouse-adapted African ZIKV strain (Dakar 41519) (Richner et al., 2017; Sapparapu et al., 2016; Zhao et al., 2016). At E13 (7 days after ZIKV challenge), maternal and fetal organs were collected from pregnant mice and evaluated for viral burden.

As observed previously in C57BL/6 male and BALB/c female mice (Richner et al., 2017), at day 49, the prM-E mRNA LNPs induced high levels of neutralizing antibodies in the serum of female C57BL/6 mice with EC50 values (half-maximal inhibition of virus infection) of 1/94,000 ± 24,000 (Figures 1B and 1C and Figures S1A and S1B) and EC90 values of ~1/5,500 ± 900 (Figures 1B and 1D). Substantial virological protection was observed in the maternal spleen (mean difference of ~2,500-fold, Figure 1E) and brain (mean difference of ~15,000-fold, Figure 1F) of mice immunized with prM-E mRNA compared to placebo mRNA LNPs. Placenta and fetal heads at E13 from placebo mRNA LNP-vaccinated dams showed high levels of viral RNA (e.g., ~10^5 to 10^8 FFU equivalents/g), whereas corresponding tissues from dams immunized with prM-E mRNA LNPs showed marked protection (placenta, 200-fold mean reduction; fetal head, 13,000-fold mean reduction) (Figures 1G and 1H). Indeed, 10 of 19 (53%) placentas and 11 of 19 (58%) fetal heads from prM-E mRNA LNPs dams had viral RNA levels at the limit of detection of the assay, suggesting virtually complete protection, and the remainder had substantially lower levels than those detected in samples from placebo mRNA LNP immunized mice. Whereas we detected infectious virus by plaque assay in 21 of 23 (91%) placentas and 10 of 23 (43%) fetal heads from placebo-vaccinated dams, only 3 of 19 (16%) placentas and 0 of 19 fetal heads were positive from dams immunized with prM-E mRNA LNPs (Figures S2A and S2B).

Protective Activity of a Live-Attenuated Virus with Mutations in NS1

We next evaluated the ability of a second vaccine platform, a live-attenuated ZIKV strain, to protect non-pregnant and pregnant mice from infection and disease. Based on strategies

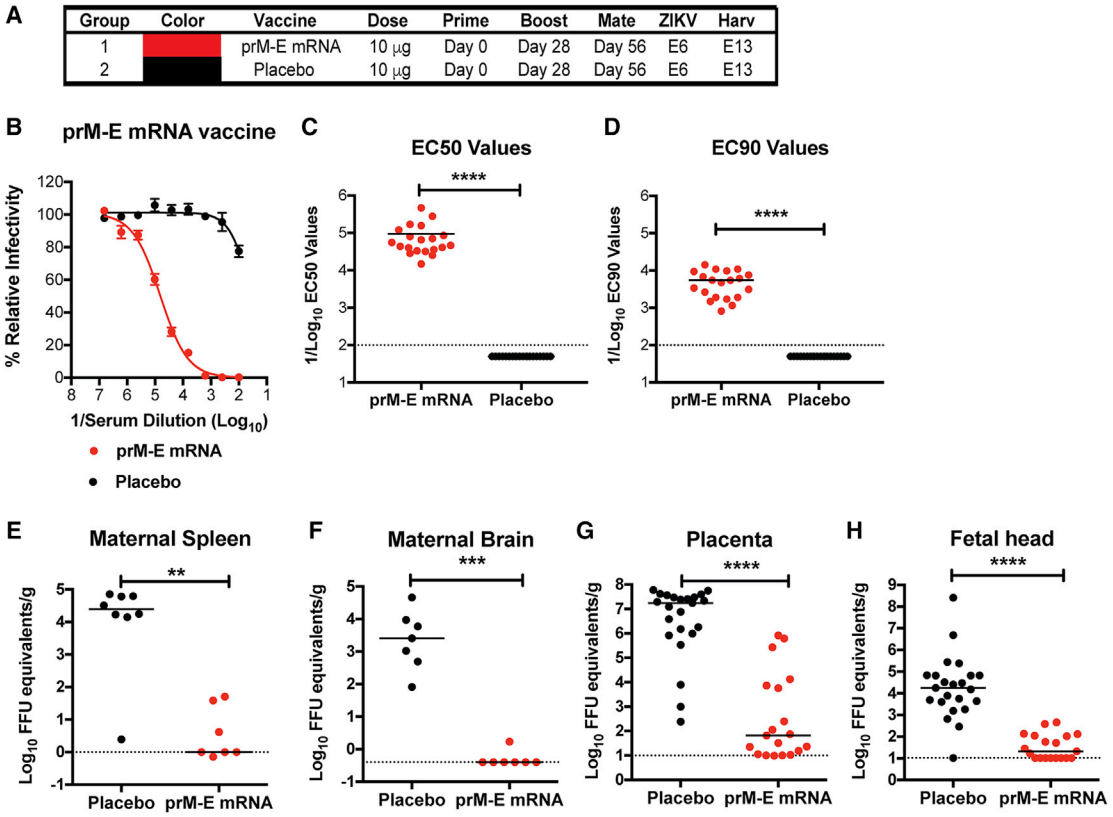

Figure 1. ZIKV prM-E mRNA LNP Vaccine Protects Pregnant C57BL/6 Mice and their Developing Fetuses

(A) Scheme of immunization and boosting of WT C57BL/6 female mice with 10 μg of prM-E or placebo mRNA LNP vaccines.

(B) Serum was collected at day 49 and analyzed for neutralizing activity (Dowd et al., 2016a). Representative neutralization curves are shown. Error bars denote the range of duplicate technical replicates.

(C and D) EC50 (C) and EC90 (D) values were calculated for individual animals in each group (n = 19 to 20). The dashed lines indicate the limit of detection of the assay. Asterisks indicate statistically significant differences (Mann-Whitney test: ****$p < 0.001$).

(E–H) At day 56, vaccinated female mice were mated with WT C57BL/6 males. A subset of the mice developed vaginal plugs, and pregnant mice (n = 7 or 8 depending on group pooled from two independent experiments) were administered 2 mg of anti-Ifnar1 blocking antibody on E5, and 1 day later (E6) challenged with 10^5 FFU of mouse-adapted ZIKV Dakar 41519. At E13, animals were euthanized and maternal spleen (E), maternal brain (F), placenta (G), and fetal heads (H) were harvested and analyzed for levels of ZIKV RNA. The dashed line indicates the limit of detection of the assay and asterisks indicate significant differences (Mann-Whitney test: **$p < 0.01$; ***$p < 0.001$; ****$p < 0.0001$).

for attenuating replication and virulence of other flaviviruses including YFV, DENV, and WNV (Muylaert et al., 1996; Pryor et al., 1998; Somnuke et al., 2011; Whiteman et al., 2010; Whiteman et al., 2011), we mutated the N-linked glycosylation sites (N130Q and N207Q) of the NS1 gene of an Asian ZIKV (FSS13025, Cambodia, 2010) infectious cDNA clone (Shan et al., 2016) to create single or double glycosylation knockout variants (Figure 2A). Four amino-acid substitutions (N130Q/S132A, and N207Q/T209V) were engineered in the double glycosylation mutant to minimize reversion and enhance safety, as described for WNV (Whiteman et al., 2011). Western blotting of infected cell lysates revealed the expected electrophoretic mobility shifts associated with loss of N-linked glycans on NS1 (Figure 2B). ZIKV with NS1 containing two glycosylation site mutations showed decreased plaque size and reduced replication in cell culture (Figures 2C–2E), with lesser attenuating effects of viruses containing one glycosylation mutation (Figures S3A and S3B). Although five serial passages of the double NS1 glycosylation mutant on Vero cells did not change the engineered substitutions as judged by consensus sequencing, an adaptive mutation (NS1-V134F) did emerge (Figure S4).

We assessed the attenuation, immunogenicity, and protective activity of the NS1 glycosylation double knockout ZIKV (ZIKV-NS1-LAV) in non-pregnant immunocompromised mice lacking type I interferon (IFN) signaling responses. Three-week-old *Ifnar1*$^{-/-}$ A129 male mice were divided into three groups, with each receiving a single subcutaneous inoculation of a placebo control (PBS), or 10^4 plaque forming units (PFU) of ZIKV-NS1-LAV, or parental WT ZIKV (Figure 2F). We monitored morbidity, mortality, and viral burden over the first 2 weeks after inoculation. Whereas mice receiving the parental infectious clone-derived WT ZIKV developed substantial weight loss (Figure 2G), death (60% mortality; Figure 2H), and viremia (10^4 to 10^7 PFU/ml at days 2 to 4 after infection; Figure 2I), ZIKV-NS1-LAV-inoculated mice sustained no weight loss or mortality, and developed less viremia (10^2 to $\sim10^4$ PFU/ml) on corresponding days. Moreover,

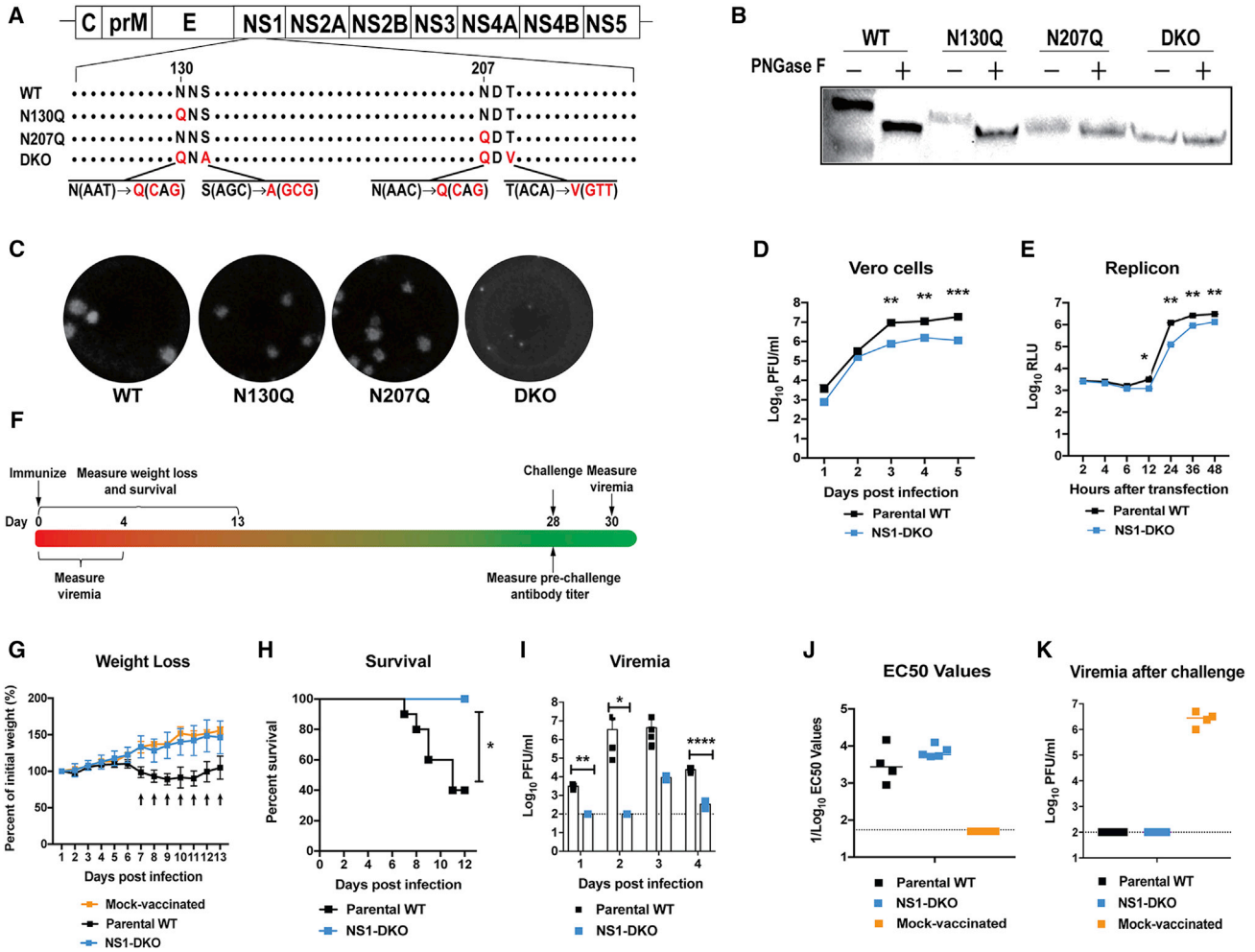

Figure 2. Development and Characterization of a Live-Attenuated ZIKV Vaccine with Mutations in the NS1 Gene

(A) Scheme of ZIKV genome with mutations in the NS1 gene. Mutated amino acids and their coding nucleotides are indicated in red.

(B) Western blotting of lysates from Vero cells infected with parental WT, N130Q, N207Q, or N130Q+S132A+N207Q+T209V (DKO) ZIKV with an anti-NS1 antibody. Where indicated, PNGase F treatment was performed on lysates to remove N-linked glycans. Results are representative of several experiments.

(C–E) Attenuated growth of ZIKV-NS1-LAV (DKO). Plaque assays (C), replication kinetics (D), and transient replicon (E) assays were performed in Vero cells. (D) Multi-step growth curves of parental WT and ZIKV-NS1-LAV in Vero cells. Results are the average of two independent experiments, and the error bars indicate standard deviations (SD). (E) Replication of parental WT or ZIKV-NS1-LAV subgenomic replicons encoding a luciferase reporter gene after transfection of in vitro derived RNA into Vero cells. Results are the average of two independent experiments, and the error bars indicate SD.

(F) Scheme of vaccination and challenge of 3-week-old *Ifnar1*$^{-/-}$ A129 male mice with parental and ZIKV-NS1-LAV.

(G and H) Weight measurements (G) and mortality (H) over the first 2 weeks after immunization with mock vaccine (G) only, n = 4), parental WT (G), n = 5: (H), n = 10) or ZIKV-NS1-LAV (n = 5). Arrows (G) and asterisks (H) indicate statistically significant differences: ((G) Two-way ANOVA with Bonferroni multiple comparison test: day 7 and 8, ***p < 0.001; days 9–12, ****p < 0.0001; day 13, **p < 0.01; (H) Log-rank test: *p < 0.05).

(I) Viremia measurements at days 1 through 4 after inoculation with parental (n = 5) and ZIKV-NS1-LAV (n = 3) as determined by plaque assay. Dotted line indicates limit of detection of assay. Asterisks indicate statistical significance (Mann-Whitney test: *p < 0.05; **p < 0.01; ****p < 0.0001).

(J) Blood was collected at day 28 and analyzed for serum neutralizing activity.

(K) A129 mice that were initially inoculated with placebo (mock-vaccinated) (n = 4), parental WT (n = 4) or ZIKV-NS1-LAV (n = 5) were challenged at day 30 with 10^6 PFU of ZIKV strain PRVABC59. At day 2 after challenge, viremia was measured.

at days 6 and 10 post-infection, viral burden in the heart, lung, liver, spleen, kidney, muscle, brain, eye, and testis was substantially lower (100 to 1,000,000-fold) in A129 mice inoculated with ZIKV-NS1-LAV compared to WT ZIKV (Figure S5). In comparison, lower levels of attenuation in A129 mice were observed with the single glycosylation mutant (N130Q or N207Q) ZIKV strains (Figures S3C–S3E). ZIKV-NS1-LAV also was attenuated in an intracranial inoculation model of outbred infant CD1 mice (50% lethal dose [LD50] of ~500 PFU for WT ZIKV compared to >10,000 PFU for ZIKV-NS1-LAV Figure S3F). Finally, we examined the ability of ZIKV-NS1-LAV to infect *Aedes aegypti* by feeding mosquitoes with artificial blood meals containing

A

Group	Color	Vaccine	Dose	Prime	Mate	Challenge	Harvest
1		LAV (NS1 DKO)	10^5 PFU	Day 0	Day 35	E6	E13
2		Placebo	None	Day 0	Day 35	E6	E13

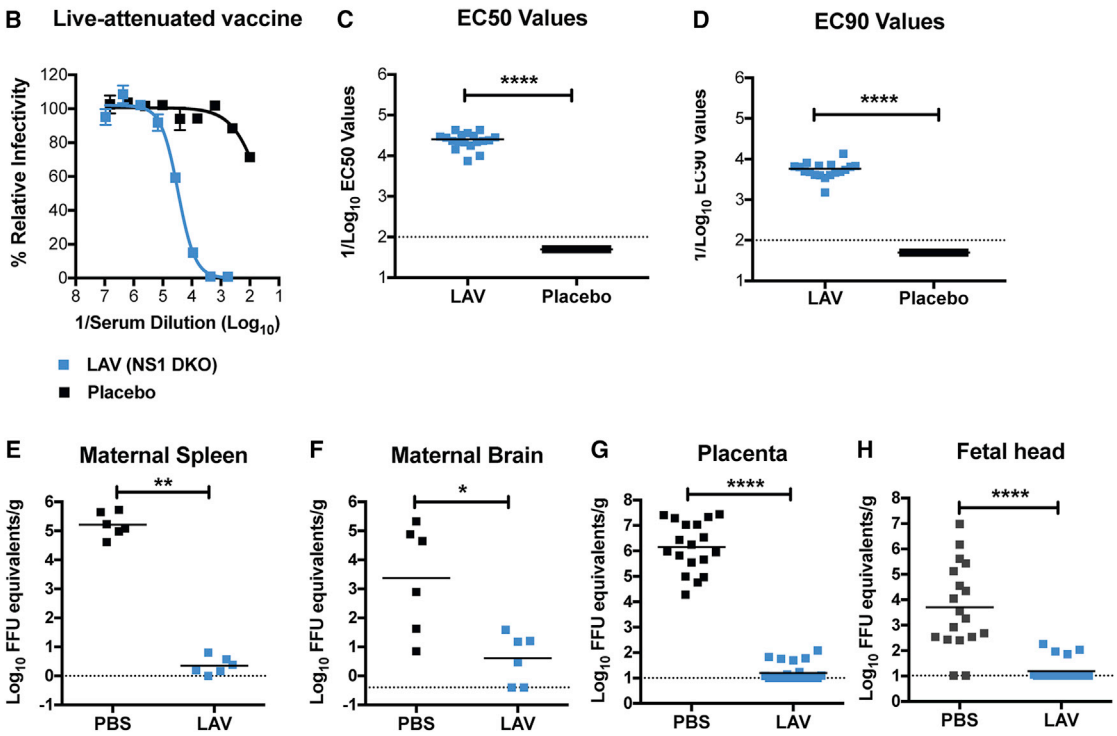

Figure 3. ZIKV-NS1-LAV Protects Pregnant C57BL/6 Mice and Their Fetuses

(A) Scheme of immunization of WT C57BL/6 female mice with 10^5 FFU of ZIKV-NS1-LAV (n = 18) or placebo (n = 11) control. One day prior to immunization, all mice were administered 0.5 mg of anti-Ifnar1.

(B) Serum was collected at day 28 and analyzed for neutralizing activity. Representative neutralization curves are shown. Error bars denote the range of duplicate technical replicates.

(C and D) EC50 (C) and EC90 (D) values were calculated for individual animals in each group. The dashed lines indicate the limit of detection of the assay. Asterisks indicate statistically significant differences (Mann-Whitney test: ****$p < 0.0001$).

(E–H) At day 35, vaccinated female mice were mated with WT C57BL/6 males. A subset of mice developed vaginal plugs (n = 6, PBS placebo; n = 6, ZIKV-NS1-LAV). Pregnant mice were challenged with ZIKV as described in Figure 1. At E13, animals were euthanized and maternal spleen (E), maternal brain (F), placenta (G), and fetal heads (H) were harvested and analyzed for levels of ZIKV RNA. The dashed line indicates the limit of detection of the assay, and asterisks indicate significant differences (Mann-Whitney test: *$p < 0.05$; **$p < 0.01$; ****$p < 0.0001$).

10^6 FFU/ml of WT parental or ZIKV-NS1-LAV. On day 7 post-feeding, the WT virus infected 56% of the engorged mosquitoes. In contrast, none of the mosquitoes were infected by ZIKV-NS1-LAV (Figure S6), suggesting that the attenuated vaccine had markedly reduced ability to infect its principal urban mosquito.

At day 28, animals were phlebotomized for analysis of serum neutralizing antibody. *Ifnar1*$^{-/-}$ A129 mice receiving either WT or ZIKV-NS1-LAV had strong neutralizing antibody responses, with EC_{50} values of ~1/5,000 to 1/7,000 (Figure 2J). After challenge with 10^6 PFU of WT ZIKV PRVABC59 (Puerto Rico 2015), A129 mice receiving the placebo control sustained high levels (10^6 to 10^7 PFU/ml) of viremia at day 2 (Figure 2K) compared to animals immunized with ZIKV-NS1-LAV or survivors of WT ZIKV infection, which had no detectable viremia at this time point.

Based on promising results in immunocompromised mice, we tested the ZIKV-NS1-LAV platform for protection during pregnancy (Figure 3A). Eight-week-old WT C57BL/6 female mice were vaccinated subcutaneously with a placebo control or 10^5 PFU of ZIKV-NS1-LAV; to facilitate transient replication of the attenuated strain in WT immunocompetent mice, we administered a single (0.5 mg) dose of anti-Ifnar1 1 day prior to virus inoculation. No signs of illness (weight loss or change in activity) were observed after infection. Twenty-eight days later, animals were bled for serological analysis, which showed high titers of neutralizing antibodies with EC50 and EC90 values of 1/25,000 ± 2,000 and 1/5,800 ± 600, respectively compared to the placebo control (Figure 3B–3D, and Figures S7A and S7B). One week later, immune female mice were mated with 12-week-old WT C57BL/6 male mice and monitored for vaginal plugs

(Figure 3A). For the challenge studies, to facilitate ZIKV dissemination to the placenta, pregnant mice were administered 2 mgs of anti-Ifnar1 at E5 1 day prior to infection (at E6) with 10^5 FFU of mouse-adapted ZIKV Dakar 41519. At E13, maternal and fetal organs were evaluated for tissue viral burden.

ZIKV-NS1-LAV conferred protection in the dams with reduced levels of virus in the spleen (~50,000-fold mean reduction, Figure 3E) and brain (~4,400-fold mean reduction, Figure 3F) compared to placebo-vaccinated animals. Placenta and fetal heads from ZIKV-NS1-LAV immunized dams also showed markedly lower levels of viral RNA (placenta, 276,000-fold mean reduction; fetal head, 20,000-fold mean reduction) than from placebo-immunized dams (Figure 3G and 3H). Indeed, 18 of 23 (78%) placentas and 19 of 23 (83%) fetal heads from ZIKV-NS1-LAV immunized dams had viral RNA levels at or below the detection limit of the assay, suggesting that the vast majority of pregnant mice did not transmit ZIKV to their developing fetuses. Consistent with this observation, infectious virus was not recovered from the placentas or fetal heads from dams immunized with ZIKV-NS1-LAV (Figures S2A and S2B, n = 23).

Vaccine Protection against Placental and Fetal Injury

The reduction in viral load mediated by prM-E mRNA LNP and ZIKV-NS1-LAV vaccines was associated with decreased damage of the placenta compared to placebo-immunized dams. The prM-E mRNA LNP and ZIKV-NS1-LAV vaccines both protected against ZIKV-induced placental insufficiency (Miner et al., 2016), as the total, labyrinth, and junctional areas of the placenta were greater than in infected animals receiving a placebo vaccine (Figure 4A and Figure 5A). In situ hybridization revealed an almost complete absence of viral RNA in the maternal decidua and the junctional zone of the placenta from animals immunized with prM-E mRNA LNP and ZIKV-NS1-LAV as compared to placebo controls (Figure 4B and Figure 5B). To determine the effects on fetal viability, we challenged prM-E mRNA vaccinated and unvaccinated (placebo) dams and followed their pregnancies through term. Whereas none of the unvaccinated dams delivered pups at term because of extensive placental injury and fetal demise, 100% of fetuses from prM-E vaccinated dams were born (Figure 4C–4E). Consistent with this result, at term, pup heads from vaccinated dams had no measurable ZIKV RNA, whereas those harvested from moribund unvaccinated dams just prior to term (E18) had high levels of viral RNA (Figure 4F). Analogously, placebo-vaccinated dams had a lower rate of fetal viability compared to animals immunized with ZIKV-NS1-LAV (Figure 5C). Collectively, the virological and histopathological data suggest that immunization with prM-E mRNA LNP or ZIKV-NS1-LAV vaccines can reduce dissemination of ZIKV to the placenta, which substantially decreases the likelihood of placental infection and injury; this prevents vertical transmission and improves fetal outcome.

DISCUSSION

There has been a rapid emergency effort to develop a safe and effective vaccine against ZIKV to limit the epidemic force of infection and prevent its major disease manifestations, such as microcephaly and congenital malformations in the context of infection during pregnancy. Recent studies have established that candidate anti-ZIKV vaccines can protect against viremia, tissue viral burden, and/or lethal challenge in mice or non-human primate models of ZIKV infection and pathogenesis (Abbink et al., 2016; Dowd et al., 2016b; Larocca et al., 2016; Muthumani et al., 2016; Pardi and Weissman, 2017; Richner et al., 2017; Shan et al., 2017a). Several of these ZIKV vaccine platforms (DNA plasmid or modified mRNA LNPs encoding prM-E gene and chemically inactivated virions) have advanced to phase 1 human trials (Durbin, 2016). However, all of the pre-clinical studies have been performed in non-pregnant animals, and thus vaccine-mediated protection against placental and fetal infection and injury has not been demonstrated. Protection should be possible, as passive transfer of ZIKV-117, a highly neutralizing human anti-ZIKV antibody, limited placental infection and transmission to the fetus (Sapparapu et al., 2016). Here, we showed that two different vaccine platforms based on Asian/American ZIKV strains, a modified mRNA LNP encoding ZIKV prM-E and a live-attenuated ZIKV with mutations in the NS1 gene, generate robust neutralizing antibody responses in female mice. After becoming pregnant, vaccinated mice were challenged at E6 with a lethal dose of a heterologous African strain of ZIKV via a subcutaneous route. Relative to the placebo controls, dams immunized with prM-E mRNA LNPs or ZIKV-NS1-LAV showed markedly diminished levels of viral RNA in maternal, placental, and fetal tissues, and the majority of fetuses showed no evidence of transmission. Thus, at least in mice, ZIKV vaccines administered before pregnancy can prevent placental and fetal infection.

Two lipid-encapsulated modified mRNA vaccines encoding the prM-E genes were recently described in the context of challenge of non-pregnant mice and non-human primates (Pardi et al., 2017; Richner et al., 2017). In the published studies in non-pregnant animals, both mRNA prM-E vaccines induced durable high-titer neutralizing antibody responses that lasted months after vaccination and conferred protection against challenge with pathogenic ZIKV strains. Because these mRNA LNP vaccines are non-amplifying, lack the capacity to integrate into the genome, and use modified nucleosides to minimize untoward innate immune activation (Pardi and Weissman, 2017; Schlake et al., 2012), there is a high safety expectation, especially in immunocompromised individuals or pregnant women, who might not be eligible to receive live-attenuated vaccines. Our study demonstrates that prM-E mRNA LNP vaccines can protect against maternal, placental, and fetal infection, with the majority of animals showing no virological evidence of transmission.

Several live-attenuated vaccines have been implemented against related flaviviruses including YFV, DENV, and JEV (Guy and Jackson, 2016; Pierson and Diamond, 2013). Recently, a live-attenuated ZIKV vaccine strain encoding a 10 nucleotide deletion in the 3′ untranslated region was shown to induce protective and sterilizing immunity against ZIKV infection in immunocompromised mice (Shan et al., 2017a); however, this vaccine was not tested in the context of challenge of pregnant animals. In our current study, a single dose of ZIKV-NS1-LAV given before pregnancy induced an immune response that protected against challenge during pregnancy with substantial reductions

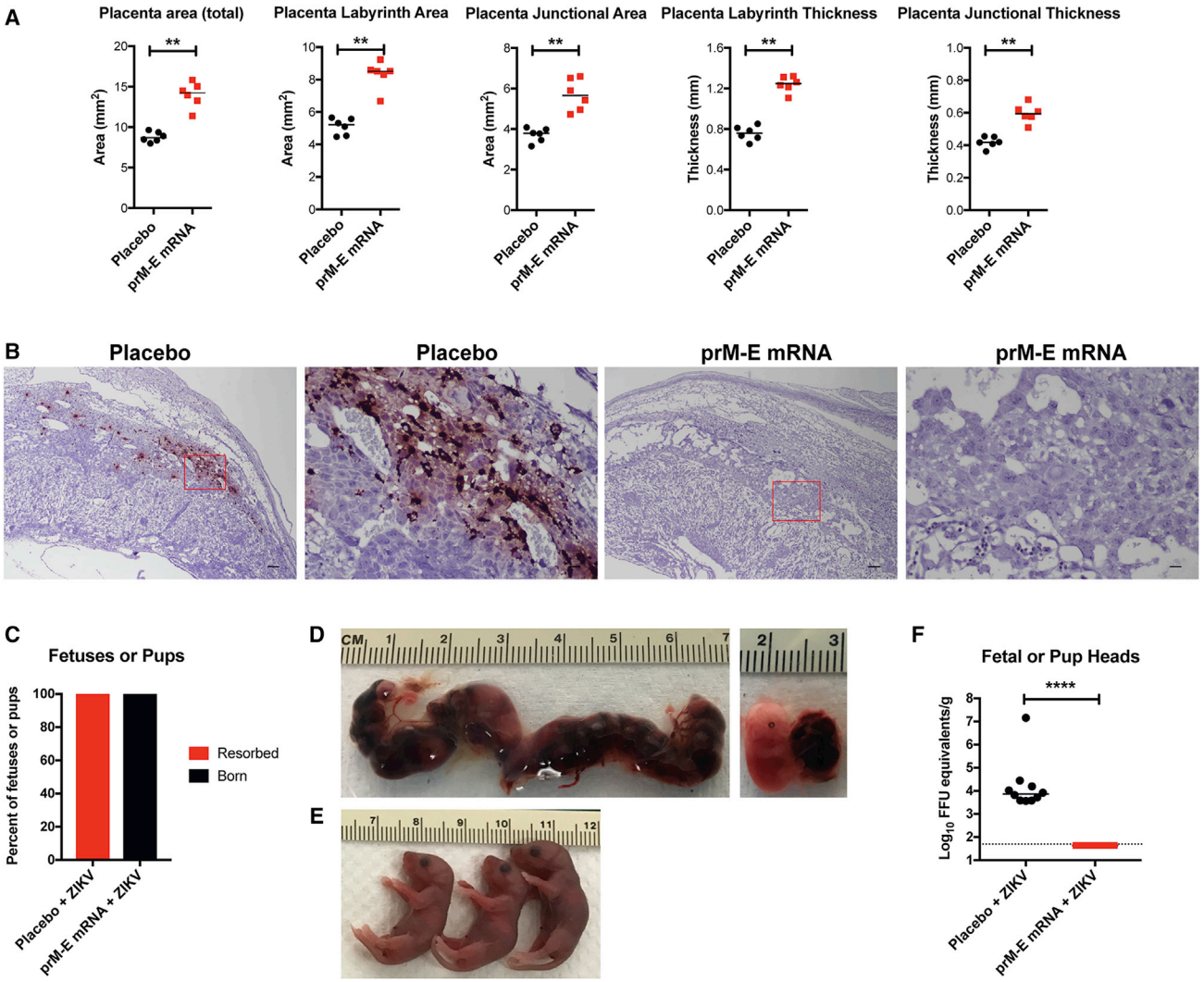

Figure 4. prM-E ZIKV Vaccine Protects against Placental and Fetal Infection

(A and B) Pregnant dams vaccinated with placebo ot prM-E mRNA LNPs were treated with anti-Ifnar1 and then inoculated with ZIKV-Dakar at E6 as described in Figure 1. (A). Measurements of thickness and indicated areas of placentas from placebo or prM-E mRNA LNPs immunized mice after ZIKV challenge. Each symbol represents data from an individual placenta. Statistical significance was analyzed (Mann-Whitney test: *$p < 0.05$; **$p < 0.01$). (B) In situ hybridization. Low power (scale bar, 100 μm) and high power (scale bar, 20 μm) images are presented in sequence (indicated with a red box) from placebo or prM-E mRNA LNPs (immunized mice after ZIKV challenge. The images in panels are representative of three to four independent placentas from multiple dams.

(C–E) Outcome of fetuses from placebo or prM-E mRNA LNP vaccinated dams. (C) The percentage of offspring that were resorbed (fetuses, prior to delivery) or delivered (pups, at term) (n = 17 for placebo; n = 14 for prM-E mRNA LNP vaccine; chi-square test (****$p < 0.0001$). (D) Representative images of grossly hemorrhagic uterus (*left*) and hypomorphic fetus and placenta (*right*) recovered from placebo-immunized moribund dams at E18. (E) Representative images of pups delivered at term to prM-E mRNA LNP vaccinated dams.

(F) Levels of viral RNA in the heads of placebo-vaccinated and ZIKV challenged (harvested from moribund dams at day E18 or by Caesarean section at term) or prM-E mRNA-vaccinated and ZIKV challenged (harvested at delivery). Each symbol represents data from an individual fetus or pup from at least two independent pregnant dams. Statistical significance was analyzed (Mann-Whitney test: ****$p < 0.0001$).

in maternal and placental viral titers, and prevention of transmission to the developing fetus. This attenuated ZIKV vaccine platform, which introduces four amino-acid substitutions and ten nucleotide changes to abolish the two N-linked glycosylation sites on the viral NS1 protein and prevent reversion, was based on a foundation of studies (Muylaert et al., 1996; Pryor et al., 1998; Somnuke et al., 2011; Whiteman et al., 2010; Whiteman et al., 2011) with other flaviviruses showing that such substitutions in NS1 are attenuating in cell culture, insects, and animals because of diminished replication rates, cytopathic effects, and immune evasion (Muller and Young, 2013).

Although both vaccine platforms showed efficacy in the context of challenge during pregnancy, some limitations were noted. Despite generating high levels of neutralizing antibody in serum, ZIKV RNA was detected in a few fetuses at E13, which may reflect some breakthrough of infection. The significance of

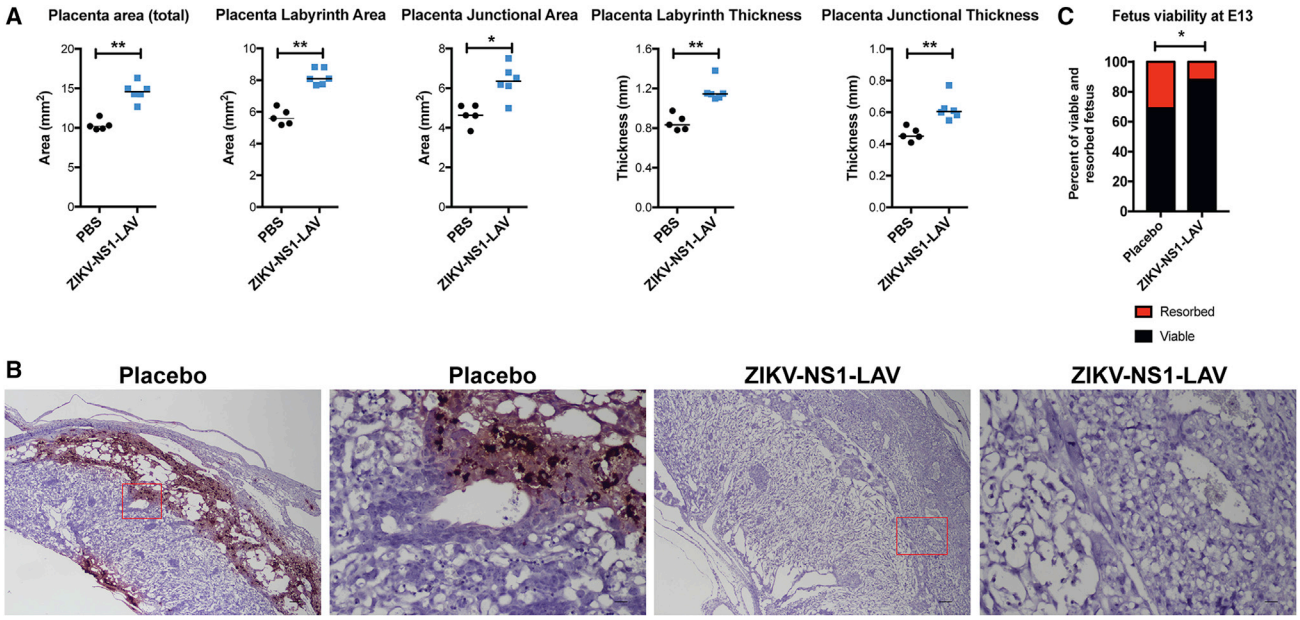

Figure 5. ZIKV-NS1-LAV Vaccine Protects against Placental and Fetal Infection

(A–C) Pregnant dams vaccinated with placebo or ZIKV-NS1-LAV were treated with anti-Ifnar1 and then inoculated with ZIKV-Dakar at E6 as described in Figure 1. (A). Measurements of thickness and indicated areas of placentas from placebo or ZIKV-NS1-LAV immunized mice after ZIKV challenge. Each symbol represents data from an individual placenta. Statistical significance was analyzed (Mann-Whitney test: *$p < 0.05$; **$p < 0.01$). (B) In situ hybridization. Low power (scale bar, 100 μm) and high power (scale bar, 20 μm) images are presented in sequence (indicated with a red box) from placebo or ZIKV-NS1-LAV immunized mice after ZIKV challenge. The images in panels are representative of three to four independent placentas from multiple dams. (C) Fetal resorption rates in placebo or ZIKV-NS1-LAV immunized dams after ZIKV challenge. Data are pooled from multiple dams in independent experiments and reflects the following number of fetuses (n = 32 for placebo and n = 48 for ZIKV-NS1-LAV). Significance for fetal survival was analyzed by the chi-square test (*$p < 0.05$).

this RNA is uncertain: 1) the levels of ZIKV RNA recovered from fetal head homogenates of prM-E mRNA and ZIKV-NS1-LAV vaccinated dams were low, and infectious virus was never recovered using plaque assays; (2) the low level of viral RNA detected in some fetuses could represent free or encapsidated RNA in neutralized virus particles; (3) the majority of dams that received the prM-E mRNA and ZIKV-NS1-LAV vaccines failed to boost their neutralizing titers (defined as > 4-fold change) 1 week after challenge with infectious ZIKV (Figures S1C and S1D and Figures S7C and S7D), suggesting that vaccine-induced immunity was sterilizing or nearly so; (4) in pups harvested at term from prM-E mRNA immunized dams, viral RNA was not detected in the head. Although it remains unclear how ZIKV from the dam disseminated to the placenta in the setting of high levels of serum neutralizing antibodies, human studies suggest that viral RNA can associate with erythrocytes in whole blood even after a protective antibody response is induced (Murray et al., 2017). Finally, as levels of neonatal Fc receptor in the mouse placenta are lower than in other mammalian species (Kim et al., 2009), reduced transport of maternal IgG into the fetus is expected (Pentsuk and van der Laan, 2009), which could result in an underestimated protection of maternal immunization.

Differences in experimental protocols limited our ability to make direct comparisons of the relative efficacy of the two vaccine platforms: (1) the immunization and challenge studies were not conducted concurrently, so differences over time in factors that shape immunity (e.g., maternal microbiome) could impact infectivity and transmission. Consistent with this idea, the mean ZIKV RNA levels in the placebo-vaccinated groups varied slightly; (2) the age of the dams at the time of challenge was different by several weeks due to the requirement for boosting with the prM-E mRNA LNP vaccine. Notwithstanding these differences, the ZIKV-NS1-LAV was associated with slightly less placental and fetal breakthrough of viral RNA. It is possible that the immune responses to subunit based and live-replicating ZIKV vaccines are not identical. Neutralizing antibody responses generated against subviral particles (Ferlenghi et al., 2001) from prM-E-based vaccines may differ qualitatively from those generated against virions (Kuhn et al., 2002) produced by live-attenuated vaccines expressing viral proteins in their native chemical environments. Moreover, because the ZIKV-NS1-LAV encodes the entire ZIKV open reading frame, it likely induces more optimal $CD4^+$ and $CD8^+$ T cell responses, due to the larger number of possible peptide epitopes for class I and class II major histocompatibility antigens.

As modified mRNA and live-attenuated vaccine platforms can mitigate in utero transmission of ZIKV in mice, their development in humans for different target populations should be considered. Where safety concerns are greatest (e.g., females during childbearing years, immunocompromised, and those with certain co-morbidities), the non-replicating prM-E mRNA LNP subunit-based vaccine may have greatest utility and shortest pathway to licensure. In comparison, live-attenuated vaccines (e.g., ZIKV-NS1-LAV) administered before sexual debut

may be associated with more rapid and long-term protection. Although our studies were focused on protection against transplacental transmission and fetal infection, the robust responses to the prM-E mRNA and ZIKV-NS1-LAV vaccines indicate they could diminish infection in other target populations and decrease the epidemic force of infection. Immunization of males may be important if the ZIKV-induced damage to the testes reported in mice (Govero et al., 2016; Ma et al., 2016; Uraki et al., 2017) becomes apparent in humans or to prevent sexual transmission. An additional consideration is whether in the context of pregnancy the systemic immunity that is generated by vaccination is sufficient to prevent local vaginal infection and spread via organs of the reproductive tract that occurs during sexual transmission (Khan et al., 2016; Shin and Iwasaki, 2013; Yockey et al., 2016). To address this issue, future studies are planned in which vaccinated pregnant mice are challenged via an intravaginal route. In summary, the modified mRNA and live-attenuated vaccine platforms generated sufficient immunity to protect against infection and disease in pregnant and non-pregnant mice. Based on these data, we believe their further evaluation to prevent congenital ZIKV syndrome in humans is warranted.

STAR★METHODS

Detailed methods are provided in the online version of this paper and include the following:

- KEY RESOURCES TABLE
- CONTACT FOR REAGENT AND RESOURCE SHARING
- EXPERIMENTAL MODEL AND SUBJECT DETAILS
  - Ethics statement
  - Mouse experiments
- METHOD DETAILS
  - Viruses and cells
  - Generation of modified mRNA and LNPs
  - Plasmid construction
  - Viral RNA transcription and transfection
  - Western blotting and glycosidase treatment
  - Measurement of viral burden
  - Mosquito infection
  - Viral RNA in situ hybridization (ISH)
  - Histology and immunohistochemistry
  - Neutralization assays
- QUANTIFICATION AND STATISTICAL ANALYSIS
- DATA AND SOFTWARE AVAILABILITY
- ADDITIONAL RESOURCES

SUPPLEMENTAL INFORMATION

Supplemental Information includes seven figures and can be found with this article online at http://dx.doi.org/10.1016/j.cell.2017.06.040.

AUTHOR CONTRIBUTION

J.M.R., B.W.J., S.H., K.A.D., C.S., C.R.F., P.F.C.V., G.C., T.C.P., H.L., T.W., S.L.R., P.-Y.S., and M.S.D. designed the experiments. A.D.B. and S.C.W. contributed to the design of safety and other experiments with ZIKV-NS1-LAV in mouse models. J.M.R., B.W.J., S.H., C.S., B.C., B.T.D.N., D.B.A.M., S.L.R., A.E.M., K.A.D., B.M.F., and E.A.C. performed the experiments. J.M.R, B.W.J., S.H., K.A.D, B.C., I.U.M., T.C.P., G.C., P.-Y.S., and M.S.D. analyzed the data. S.L.R. and S.C.W. provided key reagents. J.M.R., B.W.J., T.C.P., P.-Y.S. and M.S.D. wrote the first draft of the paper; all authors edited the manuscript.

ACKNOWLEDGMENTS

This work was supported by grants from the NIH-NIAID (R01 AI073755, R01 AI104972, and P01 AI106695 to M.S.D., R24AI120942 to S.C.W., and T32 AI007172 to B.W.J.), the NIH/NICHD (R01 HD091218 to I.U.M. and M.S.D.), the intramural program of NIH-NIAID (T.C.P), a research grant by DARPA (agreement # W911NF-13-1-0417), a Preventing Prematurity Initiative grant from the Burroughs Wellcome Fund (to I.U.M.), a Prematurity Research Initiative Investigator award (21-FY13-28)8 from the March of Dimes (to I.U.M.), and a research grant from Moderna (OTM10991). P.-Y.S. was supported by University of Texas Medical Branch (UTMB) startup award, UTMB Innovation and Commercialization award, University of Texas STARs Award, and a grant from Pan American Health Organization SCON2016-01353. P.F.C.V. was supported by the Ministry of Health of Brazil and by the grants from CNPq (process 303999/2016-0 and 440405/2016-5) and CAPES (Zika fast track project). We thank the Animal Resource Center and Sasha Azar at UTMB for their assistance in maintaining the A129 mouse breeding colony. M.S.D. is a consultant for Inbios, Visterra, and Takeda Pharmaceuticals and on the Scientific Advisory Boards of Moderna and OvaGene. S.C.W. is a consultant for Valera LLC, GeoVax, Inc. and Sanofi-Pasteur. S.H. and G.C. are employees of Valera LLC, a Moderna Venture focusing on the development of therapeutic approaches for Infectious Diseases, including ZIKV mRNA vaccines.

Received: April 5, 2017
Revised: June 19, 2017
Accepted: June 26, 2017
Published: July 13, 2017

REFERENCES

Abbink, P., Larocca, R.A., De La Barrera, R.A., Bricault, C.A., Moseley, E.T., Boyd, M., Kirilova, M., Li, Z., Ng'ang'a, D., Nanayakkara, O., et al. (2016). Protective efficacy of multiple vaccine platforms against Zika virus challenge in rhesus monkeys. Science *353*, 1129–1132.

Brasil, P., Pereira, J.P., Jr., Moreira, M.E., Ribeiro Nogueira, R.M., Damasceno, L., Wakimoto, M., Rabello, R.S., Valderramos, S.G., Halai, U.A., Salles, T.S., et al. (2016). Zika Virus Infection in Pregnant Women in Rio de Janeiro. N. Engl. J. Med. *375*, 2321–2334.

Brien, J.D., Lazear, H.M., and Diamond, M.S. (2013). Propagation, quantification, detection, and storage of West Nile virus. Curr. Protoc. Microbiol. *31*, 1, 18.

Cao-Lormeau, V.M., Blake, A., Mons, S., Lastère, S., Roche, C., Vanhomwegen, J., Dub, T., Baudouin, L., Teissier, A., Larre, P., et al. (2016). Guillain-Barré Syndrome outbreak associated with Zika virus infection in French Polynesia: a case-control study. Lancet *387*, 1531–1539.

Dick, G.W. (1952). Zika virus. II. Pathogenicity and physical properties. Trans. R. Soc. Trop. Med. Hyg. *46*, 521–534.

Dowd, K.A., DeMaso, C.R., and Pierson, T.C. (2015). Genotypic Differences in Dengue Virus Neutralization Are Explained by a Single Amino Acid Mutation That Modulates Virus Breathing. MBio *6*, e01559–e15.

Dowd, K.A., DeMaso, C.R., Pelc, R.S., Speer, S.D., Smith, A.R., Goo, L., Platt, D.J., Mascola, J.R., Graham, B.S., Mulligan, M.J., et al. (2016a). Broadly Neutralizing Activity of Zika Virus-Immune Sera Identifies a Single Viral Serotype. Cell Rep. *16*, 1485–1491.

Dowd, K.A., Ko, S.Y., Morabito, K.M., Yang, E.S., Pelc, R.S., DeMaso, C.R., Castilho, L.R., Abbink, P., Boyd, M., Nityanandam, R., et al. (2016b). Rapid development of a DNA vaccine for Zika virus. Science *354*, 237–240.

Durbin, A.P. (2016). Vaccine Development for Zika Virus-Timelines and Strategies. Semin. Reprod. Med. *34*, 299–304.

Faria, N.R., Azevedo, Rdo.S., Kraemer, M.U., Souza, R., Cunha, M.S., Hill, S.C., Thézé, J., Bonsall, M.B., Bowden, T.A., Rissanen, I., et al. (2016). Zika virus in the Americas: Early epidemiological and genetic findings. Science *352*, 345–349.

Ferlenghi, I., Clarke, M., Ruttan, T., Allison, S.L., Schalich, J., Heinz, F.X., Harrison, S.C., Rey, F.A., and Fuller, S.D. (2001). Molecular organization of a recombinant subviral particle from tick-borne encephalitis virus. Mol. Cell *7*, 593–602.

Govero, J., Esakky, P., Scheaffer, S.M., Fernandez, E., Drury, A., Platt, D.J., Gorman, M.J., Richner, J.M., Caine, E.A., Salazar, V., et al. (2016). Zika virus infection damages the testes in mice. Nature *540*, 438–442.

Guy, B., and Jackson, N. (2016). Dengue vaccine: hypotheses to understand CYD-TDV-induced protection. Nat. Rev. Microbiol. *14*, 45–54.

Heinz, F.X., and Stiasny, K. (2017). The Antigenic Structure of Zika Virus and Its Relation to Other Flaviviruses: Implications for Infection and Immunoprophylaxis. Microbiol. Mol. Biol. Rev. *81*, e00055–e16.

Khan, S., Woodruff, E.M., Trapecar, M., Fontaine, K.A., Ezaki, A., Borbet, T.C., Ott, M., and Sanjabi, S. (2016). Dampened antiviral immunity to intravaginal exposure to RNA viral pathogens allows enhanced viral replication. J. Exp. Med. *213*, 2913–2929.

Kim, J., Mohanty, S., Ganesan, L.P., Hua, K., Jarjoura, D., Hayton, W.L., Robinson, J.M., and Anderson, C.L. (2009). FcRn in the yolk sac endoderm of mouse is required for IgG transport to fetus. J. Immunol. *182*, 2583–2589.

Kuhn, R.J., Zhang, W., Rossmann, M.G., Pletnev, S.V., Corver, J., Lenches, E., Jones, C.T., Mukhopadhyay, S., Chipman, P.R., Strauss, E.G., et al. (2002). Structure of dengue virus: implications for flavivirus organization, maturation, and fusion. Cell *108*, 717–725.

Lanciotti, R.S., Kosoy, O.L., Laven, J.J., Velez, J.O., Lambert, A.J., Johnson, A.J., Stanfield, S.M., and Duffy, M.R. (2008). Genetic and serologic properties of Zika virus associated with an epidemic, Yap State, Micronesia, 2007. Emerg. Infect. Dis. *14*, 1232–1239.

Larocca, R.A., Abbink, P., Peron, J.P., Zanotto, P.M., Iampietro, M.J., Badamchi-Zadeh, A., Boyd, M., Ng'ang'a, D., Kirilova, M., Nityanandam, R., et al. (2016). Vaccine protection against Zika virus from Brazil. Nature *536*, 474–478.

Lazear, H.M., and Diamond, M.S. (2016). Zika Virus: New Clinical Syndromes and Its Emergence in the Western Hemisphere. J. Virol. *90*, 4864–4875.

Lazear, H.M., Govero, J., Smith, A.M., Platt, D.J., Fernandez, E., Miner, J.J., and Diamond, M.S. (2016). A Mouse Model of Zika Virus Pathogenesis. Cell Host Microbe *19*, 720–730.

Ma, W., Li, S., Ma, S., Jia, L., Zhang, F., Zhang, Y., Zhang, J., Wong, G., Zhang, S., Lu, X., et al. (2016). Zika Virus Causes Testis Damage and Leads to Male Infertility in Mice. Cell *167*, 1511–1524.e10.

Mansuy, J.M., Suberbielle, E., Chapuy-Regaud, S., Mengelle, C., Bujan, L., Marchou, B., Delobel, P., Gonzalez-Dunia, D., Malnou, C.E., Izopet, J., and Martin-Blondel, G. (2016). Zika virus in semen and spermatozoa. Lancet Infect. Dis. *16*, 1106–1107.

Miner, J.J., Cao, B., Govero, J., Smith, A.M., Fernandez, E., Cabrera, O.H., Garber, C., Noll, M., Klein, R.S., Noguchi, K.K., et al. (2016). Zika Virus Infection during Pregnancy in Mice Causes Placental Damage and Fetal Demise. Cell *165*, 1081–1091.

Muller, D.A., and Young, P.R. (2013). The flavivirus NS1 protein: molecular and structural biology, immunology, role in pathogenesis and application as a diagnostic biomarker. Antiviral Res. *98*, 192–208.

Murray, K.O., Gorchakov, R., Carlson, A.R., Berry, R., Lai, L., Natrajan, M., Garcia, M.N., Correa, A., Patel, S.M., Aagaard, K., and Mulligan, M.J. (2017). Prolonged Detection of Zika Virus in Vaginal Secretions and Whole Blood. Emerg. Infect. Dis. *23*, 99–101.

Muthumani, K., Griffin, B.D., Agarwal, S., Kudchodkar, S.B., Reuschel, E.L., Choi, H., Kraynyak, K.A., Duperret, E.K., Keaton, A.A., Chung, C., et al. (2016). In vivo protection against ZIKV infection and pathogenesis through passive antibody transfer and active immunisation with a prMEnv DNA vaccine. NPJ Vaccines. Published online November 10, 2016. http://dx.doi.org/10.1038/npjvaccines.2016.1021.

Muylaert, I.R., Chambers, T.J., Galler, R., and Rice, C.M. (1996). Mutagenesis of the N-linked glycosylation sites of the yellow fever virus NS1 protein: effects on virus replication and mouse neurovirulence. Virology *222*, 159–168.

Oehler, E., Watrin, L., Larre, P., Leparc-Goffart, I., Lastere, S., Valour, F., Baudouin, L., Mallet, H., Musso, D., and Ghawche, F. (2014). Zika virus infection complicated by Guillain-Barre syndrome–case report, French Polynesia, December 2013. Euro Surveill. *19*, 20720.

Pardi, N., and Weissman, D. (2017). Nucleoside Modified mRNA Vaccines for Infectious Diseases. Methods Mol. Biol. *1499*, 109–121.

Pardi, N., Hogan, M.J., Pelc, R.S., Muramatsu, H., Andersen, H., DeMaso, C.R., Dowd, K.A., Sutherland, L.L., Scearce, R.M., Parks, R., et al. (2017). Zika virus protection by a single low-dose nucleoside-modified mRNA vaccination. Nature *543*, 248–251.

Pentsuk, N., and van der Laan, J.W. (2009). An interspecies comparison of placental antibody transfer: new insights into developmental toxicity testing of monoclonal antibodies. Birth Defects Res. B Dev. Reprod. Toxicol. *86*, 328–344.

Pierson, T.C., and Diamond, M.S. (2013). Flaviviruses. In Fields Virology, D.M. Knipe and P.M. Howley, eds. (Lippincott Williams & Wilkins), pp. 747–794.

Prasad, V.M., Miller, A.S., Klose, T., Sirohi, D., Buda, G., Jiang, W., Kuhn, R.J., and Rossmann, M.G. (2017). Structure of the immature Zika virus at 9 Å resolution. Nat. Struct. Mol. Biol. *24*, 184–186.

Pryor, M.J., Gualano, R.C., Lin, B., Davidson, A.D., and Wright, P.J. (1998). Growth restriction of dengue virus type 2 by site-specific mutagenesis of virus-encoded glycoproteins. J. Gen. Virol. *79*, 2631–2639.

Rasmussen, S.A., Jamieson, D.J., Honein, M.A., and Petersen, L.R. (2016). Zika Virus and Birth Defects–Reviewing the Evidence for Causality. N. Engl. J. Med. *374*, 1981–1987.

Richner, J.M., Himansu, S., Dowd, K.A., Butler, S.L., Salazar, V., Fox, J.M., Julander, J.G., Tang, W.W., Shresta, S., Pierson, T.C., et al. (2017). Modified mRNA Vaccines Protect against Zika Virus Infection. Cell *168*, 1114–1125.e10.

Rossi, S.L., Tesh, R.B., Azar, S.R., Muruato, A.E., Hanley, K.A., Auguste, A.J., Langsjoen, R.M., Paessler, S., Vasilakis, N., and Weaver, S.C. (2016). Characterization of a Novel Murine Model to Study Zika Virus. Am. J. Trop. Med. Hyg. *94*, 1362–1369.

Sapparapu, G., Fernandez, E., Kose, N., Bin Cao, Fox, J.M., Bombardi, R.G., Zhao, H., Nelson, C.A., Bryan, A.L., Barnes, T., et al. (2016). Neutralizing human antibodies prevent Zika virus replication and fetal disease in mice. Nature *540*, 443–447.

Schlake, T., Thess, A., Fotin-Mleczek, M., and Kallen, K.J. (2012). Developing mRNA-vaccine technologies. RNA Biol. *9*, 1319–1330.

Shan, C., Xie, X., Muruato, A.E., Rossi, S.L., Roundy, C.M., Azar, S.R., Yang, Y., Tesh, R.B., Bourne, N., Barrett, A.D., et al. (2016). An Infectious cDNA Clone of Zika Virus to Study Viral Virulence, Mosquito Transmission, and Antiviral Inhibitors. Cell Host Microbe *19*, 891–900.

Shan, C., Muruato, A.E., Nunes, B.T.D., Luo, H., Xie, X., Medeiros, D.B.A., Wakamiya, M., Tesh, R.B., Barrett, A.D., Wang, T., et al. (2017a). A live-attenuated Zika virus vaccine candidate induces sterilizing immunity in mouse models. Nat. Med. *23*, 763–767.

Shan, C., Xie, X., Ren, P., Loeffelholz, M.J., Yang, Y., Furuya, A., Dupuis, A.P., 2nd, Kramer, L.D., Wong, S.J., and Shi, P.Y. (2017b). A Rapid Zika Diagnostic Assay to Measure Neutralizing Antibodies in Patients. EBioMedicine *17*, 157–162.

Sheehan, K.C., Lai, K.S., Dunn, G.P., Bruce, A.T., Diamond, M.S., Heutel, J.D., Dungo-Arthur, C., Carrero, J.A., White, J.M., Hertzog, P.J., and Schreiber, R.D. (2006). Blocking monoclonal antibodies specific for mouse IFN-alpha/beta receptor subunit 1 (IFNAR-1) from mice immunized by in vivo hydrodynamic transfection. J. Interferon Cytokine Res. *26*, 804–819.

Shi, P.Y., Tilgner, M., Lo, M.K., Kent, K.A., and Bernard, K.A. (2002). Infectious cDNA clone of the epidemic west nile virus from New York City. J. Virol. *76*, 5847–5856.

Shin, H., and Iwasaki, A. (2013). Generating protective immunity against genital herpes. Trends Immunol. *34*, 487–494.

Somnuke, P., Hauhart, R.E., Atkinson, J.P., Diamond, M.S., and Avirutnan, P. (2011). N-linked glycosylation of dengue virus NS1 protein modulates secretion, cell-surface expression, hexamer stability, and interactions with human complement. Virology *413*, 253–264.

Uraki, R., Hwang, J., Jurado, K.A., Householder, S., Yockey, L.J., Hastings, A.K., Homer, R.J., Iwasaki, A., and Fikrig, E. (2017). Zika virus causes testicular atrophy. Sci. Adv. *3*, e1602899.

Whiteman, M.C., Li, L., Wicker, J.A., Kinney, R.M., Huang, C., Beasley, D.W., Chung, K.M., Diamond, M.S., Solomon, T., and Barrett, A.D. (2010). Development and characterization of non-glycosylated E and NS1 mutant viruses as a potential candidate vaccine for West Nile virus. Vaccine *28*, 1075–1083.

Whiteman, M.C., Wicker, J.A., Kinney, R.M., Huang, C.Y., Solomon, T., and Barrett, A.D. (2011). Multiple amino acid changes at the first glycosylation motif in NS1 protein of West Nile virus are necessary for complete attenuation for mouse neuroinvasiveness. Vaccine *29*, 9702–9710.

Yang, Y., Shan, C., Zou, J., Muruato, A.E., Bruno, D.N., de Almeida Medeiros Daniele, B., Vasconcelos, P.F., Rossi, S.L., Weaver, S.C., Xie, X., and Shi, P.Y. (2017). A cDNA Clone-Launched Platform for High-Yield Production of Inactivated Zika Vaccine. EBioMedicine *17*, 145–156.

Yockey, L.J., Varela, L., Rakib, T., Khoury-Hanold, W., Fink, S.L., Stutz, B., Szigeti-Buck, K., Van den Pol, A., Lindenbach, B.D., Horvath, T.L., and Iwasaki, A. (2016). Vaginal Exposure to Zika Virus during Pregnancy Leads to Fetal Brain Infection. Cell *166*, 1247–1256.e4.

Zhao, H., Fernandez, E., Dowd, K.A., Speer, S.D., Platt, D.J., Gorman, M.J., Govero, J., Nelson, C.A., Pierson, T.C., Diamond, M.S., and Fremont, D.H. (2016). Structural Basis of Zika Virus-Specific Antibody Protection. Cell *166*, 1016–1027.

STAR★METHODS

KEY RESOURCES TABLE

REAGENT or RESOURCE	SOURCE	IDENTIFIER
Antibodies		
MAR1-5A3 (anti-IFNAR1)	Leinco	I-401; RRID: AB_2491621
WNV E60 (anti-E, fusion loop specific)	Diamond Laboratory	N/A
horseradish peroxidase conjugated goat anti-mouse IgG	Abcam	Ab97023; RRID: AB_10679675
horseradish peroxidase conjugated goat anti-rabbit IgG	Abcam	Ab6721; RRID: AB_955447
mouse monoclonal antibody (mAb) 4G2	ATCC	ATCC HB-112; RRID: CVCL_J890
Mouse Anti-Zika (African) NS1 Protein IgG1	Alpha Diagnostic International	Cat# ZNS112-BTN
Anti-Mouse IgG (H+L) Antibody Horseradish Peroxidase-labeled	KPL, Gaithersburg, MD	Cat# 5450-0011
goat anti-mouse IgG conjugated with Alexa Fluor488	Thermo Fisher Scientific	Cat#: A-11001; RRID: AB_2534069
Bacterial and Virus Strains		
ZIKV strain FSS13025 (with NS1 mutations)	Shi Laboratory	N/A
ZIKV strain Dakar 41519	World Reference Center for Emerging Viruses and Arboviruses, Galveston TX (UTMB)	N/A
ZIKV strain PRVABC59	World Reference Center for Emerging Viruses and Arboviruses, Galveston TX (UTMB)	N/A
ZIKV strain Dakar 41519 (mouse-adapted)	Diamond Laboratory	N/A
One Shot TOP10 Chemically Competent E. coli	Thermo Fisher Scientific	Cat#C404003
Biological Samples		
ZIKV Reporter Virus Particles (GFP)	Pierson Laboratory; Dowd, et al., 2015	N/A
ZIKV mCherry Reporter Virus Particles	Shi laboratory; Shan, et al., 2017a.	N/A
Chemicals, Peptides, and Recombinant Proteins		
RIPA Lysis Buffer	Thermo Fisher	89900
PNGAse F	New England BioLabs	P0704S
Renilla Luciferase Assay System	Promega	E2820
Critical Commercial Assays		
RNeasy Mini Kit	QIAGEN	74104
Plasmid Plus Maxi Kit	QIAGEN	12943
QIAprep Spin Miniprep Kit	QIAGEN	27106
T7 mMessage mMachine Kit	Ambion	AM1344
QIAmp viral RNA Mini Kit	QIAGEN	52904
SuperScript III One Step RT-PCR	Invitrogen	12574030
Experimental Models: Cell Lines		
Vero cells	ATCC	CCL-81
Experimental Models: Organisms/Strains		
C57BL/6 mice	Jackson Laboratory	000664
A129 mice	Rossi Laboratory	
CD-1	Charles River	24101176
Oligonucleotides		
1183F: 5′-CCACCAATGTTCTCTTGCAGACATA TTG-3′;	IDT	N/A
1268R: 5′-TTCGGACAGCCGTTGTCCAACACAAG-3′;	IDT	N/A

(*Continued on next page*)

Continued

REAGENT or RESOURCE	SOURCE	IDENTIFIER
(1213F):5′-56-FAM/AGCCTACCT TGACAAGCAGTC/ 3IABkFQ-3′.	IDT	N/A
NotI-1466-F: 5′-tctgcggccgcTAGAGCGAAGGTT GAGATAAC-3′	IDT	N/A
ClaI-3881-C: 5′-cgaatcgatACACGAGGCCAAGGCC AGCAG-3′	IDT	N/A
NS1-N130Q-F: AGGGCAGCAAAGACAcagAACAGC TTTGTCGTG	IDT	N/A
NS1-N130Q-R: 5′-CACGACAAAGCTGTTctgTGTCT TTGCTGCCCT-3′	IDT	N/A
NS1-N207Q-F: 5′-ATTGAGAGTGAGAAGcagGACA CATGGAGGCTG-3′	IDT	N/A
NS1-N207Q-R: 5′-CAGCCTCCATGTGTCctgCTTCT CACTCTCAAT-3′	IDT	N/A
NS1-130-132-F: 5′-AGGGCAGCAAAGACAcagAAC gcgTTTGTCGTGGATGGT-3′	IDT	N/A
NS1-130-132-R: 5′-ACCATCCACGACAAAcgcGTTctg TGTCTTTGCTGCCCT-3′	IDT	N/A
NS1-207-209-F: 5′-ATTGAGAGTGAGAAGcagGACgtt TGGAGGCTGAAGAGG-3′	IDT	N/A
NS1-207-209-R: 5′-CCTCTTCAGCCTCCAaacGTCctg CTTCTCACTCTCAAT-3′	IDT	N/A
Recombinant DNA		
pFLZIKV and NS1 mutants	Shi Laboratory; Shan et al., 2016	N/A
Other		
mRNA LNP vaccines (ZIKV and controls)	Valera/Moderna; Richner et al., 2017	N/A
TransBlot Turbo	BioRad	N/A
RNAScope 2.5 ISH	Advanced Cell Diagnostics	N/A
ZIKV ISH Probe	Advanced Cell Diagnostics	467771

CONTACT FOR REAGENT AND RESOURCE SHARING

Request for data or reagents should be directed and will be fulfilled by the Lead Contact, Michael S. Diamond (diamond@wusm.wustl.edu).

EXPERIMENTAL MODEL AND SUBJECT DETAILS

Ethics statement

This study was carried out in strict accordance with the recommendations in the Guide for the Care and Use of Laboratory Animals of the National Institutes of Health. The protocols were approved by the Institutional Animal Care and Use Committee (IACUC) at the Washington University School of Medicine (Assurance Number: A3381-01), the IACUC at the University of Texas Medical Branch (Protocol Number 0209068B). Dissections and footpad injections were performed under anesthesia that was induced and maintained with ketamine hydrochloride and xylazine or isofluorane, and all efforts were made to minimize suffering.

Mouse experiments

C57BL/6J mice were purchased from The Jackson Laboratory, and A129 (*Ifnar1*$^{-/-}$) mice were bred in the animal facilities at University of Texas Medical Branch. All mice were housed in pathogen-free mouse facilities. For immunizations, mice were inoculated via an intramuscular route with 50 μL of modified mRNA vaccine encoding the prM-E genes of ZIKV (Micronesia 2007) (Richner et al., 2017) or placebo non-coding mRNA or via subcutaneous route in the footpad with 10^5 PFU of a live attenuated ZIKV (strain FSS13025, Cambodia 2010) encoding mutations in the NS1 gene or PBS placebo control; the latter immunizations were performed 1 day after intraperitoneal administration of 0.5 mg of anti-Ifnar1 (MAR1-5A3) (Sheehan et al., 2006), which was purchased (Leinco, Inc). For challenge studies in A129 mice, immunized animals were inoculated subcutaneously with 10^6 PFU of ZIKV PRVABC59. Immunized

WT C57BL/6 female were mated with naive WT male mice; at E5, pregnant dams were treated with a 2 mg injection of anti-Ifnar1. At E6, mice were inoculated with 10^5 FFU of mouse-adapted ZIKV-Dakar by subcutaneous injection in the footpad. Animals were sacrificed at E13, and placentas, fetuses, and maternal tissues were harvested. To assess the impact of vaccination with prM-E mRNA LNPs on fetus survival, vaccinated or unvaccinated (placebo) WT mice were subjected to superovulation after intraperitoneal injection of 2.5 IU pregnant mare serum gonadotropin (National Hormone and Peptide Program) followed by 2.5 IU human chorionic gonadotropin (Sigma-Aldrich) 48 hr later. Female mice then were mated to 12-week-old WT males, and plugged dams were inoculated with 10^5 FFU of mouse-adapted ZIKV-Dakar at E6. Pregnant dams were monitored every 8 hr near term (E19) until all pups were delivered, and pup heads were harvested immediately for viral analysis. Moribund females were sacrificed and fetal sacs were dissected for tissue recovery and viral analysis.

Virulence of attenuated viruses was determined by performing experiments on 3-week-old A129 mice, a model susceptible to ZIKV infection (Rossi et al., 2016). A129 mice were inoculated subcutaneously with 10^4 PFU of WT or NS1 mutant viruses. Mice monitored daily for weight change and signs of disease. Mice were bled via the retro-orbital sinus to quantify the viremia using plaque assay on Vero cells. On day 28 post-immunization, mice were anesthetized and bled to measure serum antibody neutralization titers. Mice were challenged on day 30 with 10^6 PFU of ZIKV strain PRVABC59 via intraperitoneal injection. On day 2 post-challenge, the mice were bled to measure viremia.

METHOD DETAILS

Viruses and cells

ZIKV strain Dakar 41519 (Senegal, 1984), FSS13025 (Cambodia, 2007), and PRVABC59 (Puerto Rico, 2015) were provided by the World Reference Center for Emerging Viruses and Arboviruses (University of Texas Medical Branch). To create a mouse-adapted more pathogenic variant of ZIKV Dakar 41519, it was passaged twice in *Rag1*$^{-/-}$ mice (Sapparapu et al., 2016; Zhao et al., 2016). Virus stocks were propagated in mycoplasma-free Vero cells and titrated by focus-forming (FFA) or plaque assays, as described previously (Brien et al., 2013; Lazear et al., 2016). Experiments with ZIKV were conducted under biosafety level 2 (BSL2) and A-BSL3 containment with Institutional Biosafety Committee approval.

Generation of modified mRNA and LNPs

The modified mRNA encoding the ZIKV prM and E genes from an Asian ZIKV strain (Micronesia 2007, GenBank accession number EU545988 (Lanciotti et al., 2008)), which is > 99% identical to circulating American strains, has been described previously (Richner et al., 2017). Briefly, the mRNA was synthesized in vitro using T7 polymerase-mediated DNA-dependent RNA transcription where the UTP was substituted with 1-methylpseudoUTP, using a linearized DNA template, which incorporates 5′ and 3′ untranslated regions (UTRs) and includes a poly-A tail. A donor methyl group S-adenosylmethionine was added to the methylated capped RNA, resulting in a cap 1 structure to increase mRNA translation efficiency. The modified mRNAs encoded the signal sequences from human IgE.

LNP formulations were prepared as described previously (Richner et al., 2017). Briefly, lipids were dissolved in ethanol at molar ratios of 50:10:38.5:1.5 (ionizable lipid: DSPC: cholesterol: PEG-lipid). The lipid mixture was combined with mRNA at a ratio of 3:1 (aqueous:ethanol) using a microfluidic mixer (Precision Nanosystems). Formulations were dialyzed against PBS (pH 7.4), concentrated using Amicon Ultra Centrifugal Filters (EMD Millipore), passed through a 0.22-μm filter and stored at 4°C until use. All formulations were tested for particle size, RNA encapsulation, and endotoxin and were found to be between 80 to 100 nm in size, with greater than 90% encapsulation and < 1 EU/ml of endotoxin.

Plasmid construction

The NS1 single and double glycosylation mutations (N130Q, N207Q, and N130Q + S132A + N207Q + T209V) were introduced to the full-length ZIKV cDNA infectious clone pFLZIKV (Shan et al., 2016). A shuttle vector spanning nucleotide position 1,466-3,881 (GenBank number KU955593.1) was used to introduce NS1 mutations by corresponding primers using QuickChange II XL Site-Directed Mutagenesis Kit (Agilent Technologies). The shuttle vector was digested and ligated to pFLZIKV using unique restriction enzyme sites AvrII and SphI. *E. coli* strain Top 10 cells (Invitrogen) were used to propagate the plasmids. The shuttle vector and full-length plasmids were validated by DNA sequencing. All restriction enzymes were purchased from New England BioLabs.

Viral RNA transcription and transfection

The infectious cDNA plasmid with desired mutations were amplified in *E. coli* Top 10 cells, and purified using QIAGEN Plasmid Plus Maxi Kit. ZIKV NS1 mutant genomic RNAs were in vitro transcribed using a T7 mMessage mMachine kit (Ambion) from the cDNA plasmids pre-linearized by restriction enzyme ClaI. The RNA was precipitated with lithium chloride, washed with 70% ethanol, re-suspended in RNase-free water, quantitated by spectrophotometry, and stored at −80°C in aliquots. The RNA transcripts (10 μg) were electroporated into Vero cells following a protocol described previously (Shi et al., 2002). Viral RNA in cell culture media was extracted using QIAamp viral RNA Mini Kit (QIAGEN). The NS1 region was amplified from viral RNA using SuperScript III One-Step RT-PCR System with Platinum *Taq* High Fidelity (Invitrogen); the RT-PCR products were verified for the engineered mutations by DNA sequencing.

Western blotting and glycosidase treatment

Vero cells were seeded in a T-175 flask (1.75×10^7 cells/flask), inoculated with ZIKV at an MOI of 0.01, and incubated at 37°C until cytopathic effect began to appear. The infected cells were harvested, washed with cold PBS, and lysed with RIPA buffer. The lysed cells were placed on a Fisher Scientific Mini-Tube Rotator for a gentle agitation for 1 hr at 4°C. The lysates were centrifuged at 21,130 × g for 10 min at 4°C to remove cell debris. Aliquots of cell lysates were treated with Peptide N-Glycosidase F (PNGase F) in accordance to the manufacturer's instructions (New England BioLabs.). Proteins was analyzed under denaturing conditions in 12% SDS-polyacrylamide gel electrophoresis (SDS-PAGE), and transferred using a Trans-Blot Turbo Blotting System (Bio-Rad Laboratories) onto polyvinylidene difluoride (PVDF) membranes. Blots were blocked in TBST buffer (10 nM Tris-HCl, PH 7.5, 150 nM NaCl, and 0.1% Tween 20) supplemented with 5% skim milk for 1 hr, followed by probing with primary antibodies (1:2000 dilution) for 1 hr at room temperature. After two washes with TBST buffer, the blots were incubated with goat anti-rabbit conjugated to HRP (1:5,000 dilution) in TBST buffer with 5% milk for 1 hr, followed by three washes with TBST buffer. Amersham ECL Prime Western Blotting detection reagent (GE Healthcare) was used to generate chemiluminescence signals which were detected by Chemi Doc Touch imaging system (Bio-Rad).

Measurement of viral burden

At E13 (7 days after ZIKV challenge), maternal blood was collected and organs from dams (brain and spleen) and fetuses (placenta and fetal head) were recovered. Organs were weighed and homogenized using a bead-beater apparatus (MagNA Lyser, Roche), and serum was prepared after coagulation and centrifugation. Tissue samples and serum from ZIKV-infected mice were extracted with the RNeasy Mini Kit (QIAGEN). ZIKV RNA levels were determined by TaqMan one-step quantitative reverse transcriptase PCR (qRT-PCR) on an ABI 7500 Fast Instrument using standard cycling conditions. Viral burden is expressed on a $\log_{10}$ scale as viral RNA equivalents per gram or per milliliter after comparison with a standard curve produced using serial 5-fold dilutions of ZIKV RNA from known quantities of infectious virus. For ZIKV, the following primer sets were used: 1183F: 5′-CCACCAATGTTCTCTTGCAGACA TATTG-3′; 1268R: 5′-TTCGGACAGCCGTTGTCCAACACAAG-3′; and probes (1213F): 5′-56-FAM/AGCCTACCT TGACAAGCA GTC/3IABkFQ-3′. With some samples, viral burden was determined by plaque assay on Vero cells (Miner et al., 2016).

Mosquito infection

Aedes aegypti mosquitoes were collected and colonized from Galveston, Texas. Blood meal feeding of mosquitoes was performed as previously described (Yang et al., 2017). Briefly, blood meals [containing 1% (wt/vol) sucrose, 20% (vol/vol) FBS, 5 mM ATP, 33% (vol/vol) PBS-washed human blood cells (UTMB Blood Bank), and 33% (vol/vol) DMEM medium] were spiked with 10^6 FFU/ml of ZIKV. The blood meals were loaded into Hemotek 2 mL heated reservoirs (Discovery Workshops) covered with mouse skin. Mosquitoes were allowed to feed on the blood meal for 30 min. Engorged mosquitoes were incubated at 28°C, 80% relative humidity on a 12:12 hr light-dark cycle with ad libitum access to 10% sucrose. On day 7, mosquitoes were homogenized (Retsch MM300 homogenizer, Retsch Inc) individually in 500 μL of DMEM with 20% FBS and 250 μg/ml amphotericin B. The samples were centrifuged, after which 75 μL of supernatants were inoculated onto nearly confluent Vero cells in a 96-well plate. The plate was incubated at 37°C and 5% CO_2 for 3 days and analyzed for viral protein expression using an immunofluorescence assay. Mosquito infection rate was calculated by dividing the number of virus-positive mosquito by the number of engorged mosquitoes.

Viral RNA in situ hybridization (ISH)

RNA ISH was performed with RNAscope 2.5 Brown (Advanced Cell Diagnostics) according to the manufacturer's instructions, and as previously described (Sapparapu et al., 2016). Paraformaldehyde-fixed paraffin-embedded tissue sections were incubated for 60 min at 60°C and deparaffinized in xylene. Endogenous peroxidases were quenched with H_2O_2 for 10 min at room temperature. Slides were boiled for 15 min in RNAscope Target Retrieval Reagents and incubated for 30 min in RNAscope Protease Plus solution before probe hybridization. The probe targeting ZIKV RNA was designed and synthesized by Advanced Cell Diagnostics (Catalog no. 467771); specificity of ZIKV probe binding was confirmed by parallel hybridization of positive (Mm Ppib, Catalog no. 313911) and negative (dapB, Catalog no. 310043) control probes in sequential tissue sections. Tissues were counterstained with Gill's hematoxylin and visualized with standard bright-field microscopy (Nikon Eclipse E400).

Histology and immunohistochemistry

Harvested placentas were fixed in 10% neutral buffered formalin at room temperature and embedded in paraffin. At least three placentas from different litters with the indicated treatments were sectioned and stained with hematoxylin and eosin to assess morphology. Surface area and thickness of placenta and different layers were measured using ImageJ software.

Neutralization assays

(a) GFP Reporter virus particles (RVPs). RVPs incorporating the structural proteins of ZIKV were produced by complementation of a previously described sub-genomic GFP-expressing replicon derived from a lineage II strain of WNV (Dowd et al., 2016a; Dowd et al., 2015). Serial dilutions of heat-inactivated sera obtained from immunized C57BL/6J mice were mixed with ZIKV (strain H/PF/2013; French Polynesia, 2013) RVPs and incubated for 1 hr at 37°C. Immune complexes were added in duplicate technical replicates to pre-plated Vero cells in a 96-well plate and incubated for 2 days. Cells were trypsinized, resuspended in 4% paraformaldehyde in

PBS, and RVP infection scored as a function of GFP expression by flow cytometry. All neutralization data were analyzed by non-linear regression to determine the dilution of sera required to inhibit 50% (EC50) and 90% (EC90) of infection. (b) mCherry ZIKV. For serum generated in A129 mice, neutralizing activity was assessed using an mCherry reporter ZIKV infection assay (Shan et al., 2017b). The mCherry gene was engineered into the ZIKV Cambodian strain FSS13025 infectious clone using a strategy previously described for the Renilla luciferase gene (Shan et al., 2016). The sera were serially diluted 2-fold starting at 1:100 in DMEM with 2% FBS and 1% penicillin/streptomycin and incubated with mCherry ZIKV at 37°C for 2 hr. Antibody-virus complexes were added to pre-seeded Vero cells in 96-well plates. At 48 hr post-infection, cells were visualized by fluorescence microscopy using Cytation 5 Cell Imaging Multi-Mode Reader (Biotek) to quantify the mCherry-positive cells. The percentage of mCherry positive cells in the non-treatment controls was set at 100%. The mCherry-positive cells from serum-treated wells were normalized to those of non-treatment controls. A four-parameter sigmoidal (logistic) model (GraphPad Prism 7) was used to calculate the neutralization titers.

QUANTIFICATION AND STATISTICAL ANALYSIS

All data were analyzed with GraphPad Prism software. Kaplan-Meier survival curves were analyzed by the log rank test, and weight losses were compared using two-way ANOVA with Bonferroni multiple comparison test. For neutralization antibody titers and viral burden analysis, the log titers and levels of viral RNA were analyzed by a Mann-Whitney test or Kruskal-Wallis two-way ANOVA with a multiple comparisons correction. Fetal resorption rates were analyzed by a chi-square test. Paired antibody titer values were analyzed for differences by a Wilcoxon matched paired sign-rank test.

DATA AND SOFTWARE AVAILABILITY

All data are available upon request to the lead contact author. No proprietary software was used in the data analysis.

ADDITIONAL RESOURCES

mRNA LNP vaccines are available from Valera/Moderna upon request and completion of a Material Transfer Agreement. ZIKV-NS1-LAV is available from P-Y. Shi and University of Texas Medical Branch upon completion of a Material Transfer Agreement.

Cell

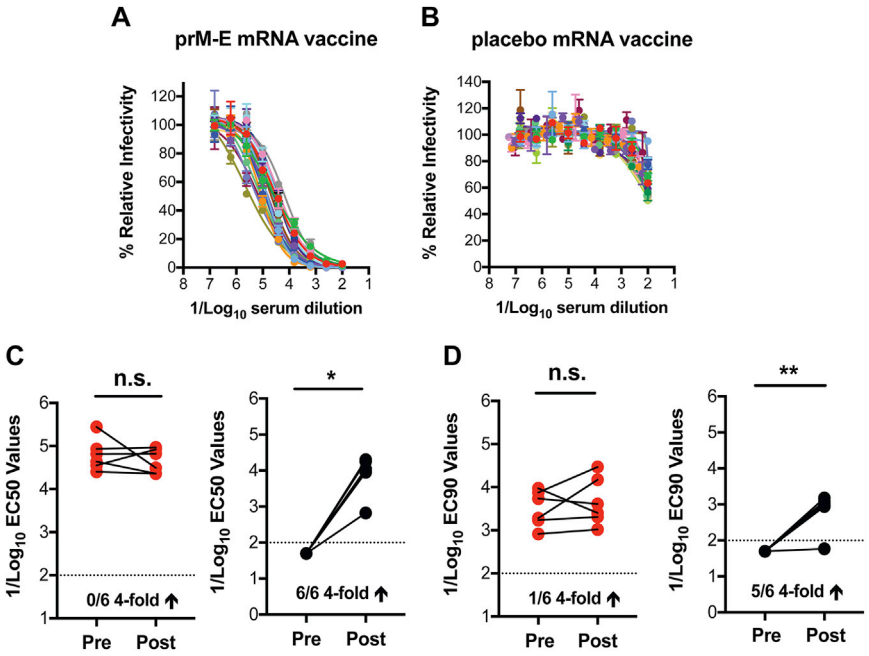

Figure S1. Neutralizing Activity of Serum from prM-E Vaccinated C57BL/6 Female Mice, Related to Figure 1

(A and B) Female C57BL/6 mice (n = 20) in each group were immunized with 10 μg of prM-E (Group 1, (A) or placebo (Group 2, (B) mRNA LNPs. Mice were boosted 28 days later. Serum was collected at day 49 post initial vaccination and analyzed for neutralizing activity of ZIKV. Each line represents the neutralization curve from an individual mouse.

(C and D) Anamnestic neutralizing antibody response. Paired sera were collected from vaccinated animals (prM-E or placebo mRNA) before (Pre) or 7 days after (Post) ZIKV challenge (only pregnant animals shown) and analyzed for neutralizing activity. EC50 (C) and EC90 (D) values were analyzed for differences by a Wilcoxon matched paired sign-rank test (n.s., not significant; *$p < 0.05$; **$p < 0.01$). Indicated at the bottom of each graph is the number of animals showing a 4-fold increase in neutralization titer at 7 days after ZIKV challenge.

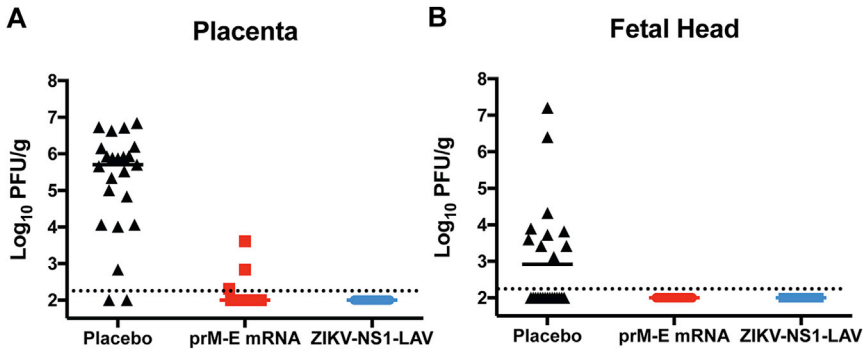

Figure S2. Infectious Viral Titers in the Placenta and Fetal Heads, Related to Figures 1 and 3

(A and B) Placenta (A) and fetal heads (B) were collected at day 7 after challenge (E13) from placebo, prM-E mRNA LNP, and ZIKV-NS1-LAV immunized mice and tested for infectious virus by plaque assay. Dashed lines indicate limit of detection of the assays. Results are pooled from two independent biological experiments, and each symbol represents data from an individual placenta or fetus (n = 19 to 23). Bars indicate median values.

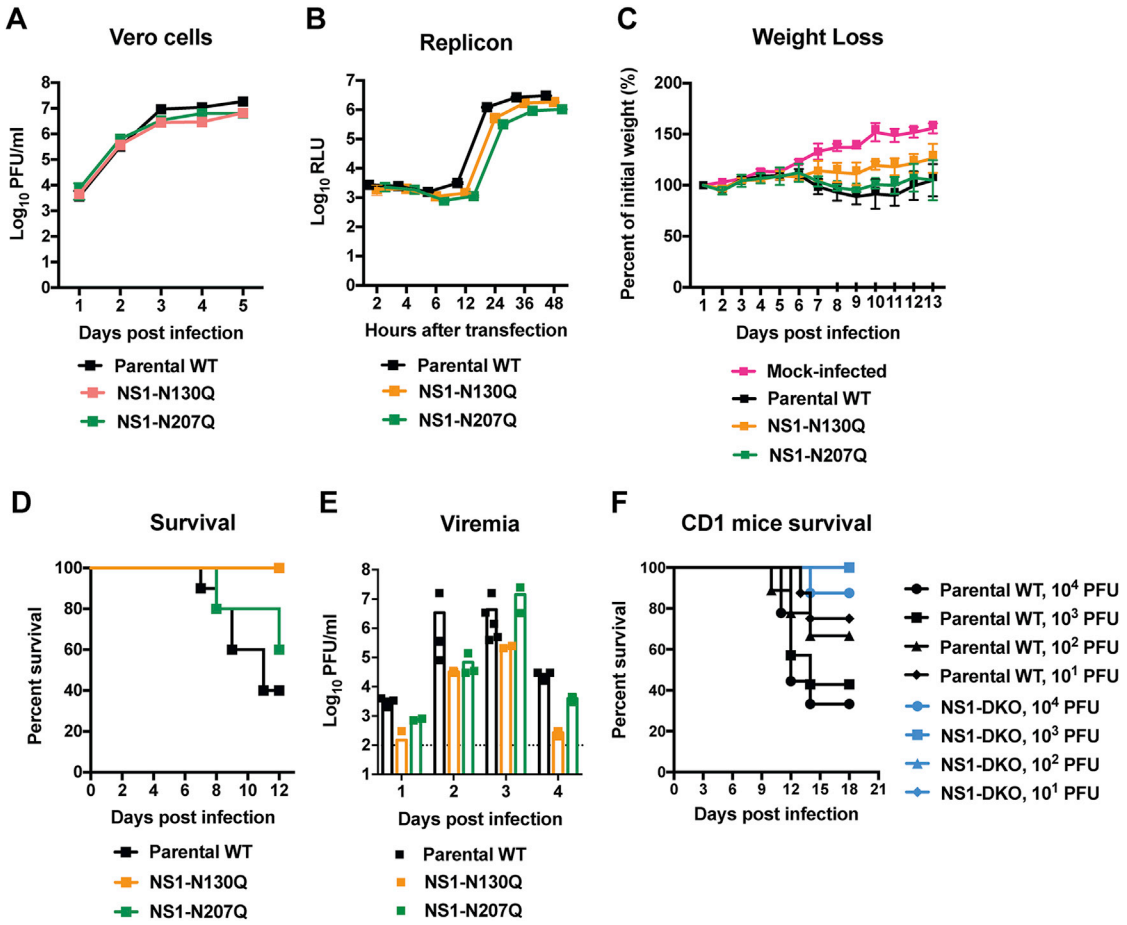

Figure S3. Effects of Single Mutations in NS1 on ZIKV Infectivity and Pathogenesis, Related to Figure 2

(A and B) Growth of ZIKV-NS1-N130Q and ZIKV-NS1-N207Q in Vero cells. (A) Multi-step growth curve of parental and NS1 mutant ZIKV in Vero cells. Results are from two independent experiments, and the error bars indicate SD (B) Replication of parental WT and NS1 mutant ZIKV subgenomic replicons encoding a luciferase reporter gene after transfection of in vitro derived RNA into Vero cells. Results are from two independent experiments, and the error bars indicate SD. (C–E) Challenge of 3-week-old *Ifnar1*$^{-/-}$ A129 male mice with parental WT and NS1 mutant ZIKV. Weight measurements (C) and mortality (D) over the first 2 weeks after infection with mock infection (C) only, n = 4), parental WT (C), n = 5: (D), n = 10), ZIKV-NS1-N130Q (C), n = 5: (D), n = 5), or ZIKV-NS1-N207Q (C), n = 5: (D), n = 5). (E). Viremia measurements at days 1 through 4 after infection with parental (n = 5), ZIKV-NS1-N130Q (n = 3), and ZIKV-NS1-N207Q (n = 3) as determined by plaque assay. Dotted line indicates limit of detection of assay. For (A–E), the WT parental ZIKV data correspond to that shown in Figure 3, as the experiments were performed concurrently.

(F) Survival studies in 1-day-old CD1 outbred mice. The indicated amounts of parental WT or ZIKV-NS1-LAV (DKO) (n = 6 to 9 mice per group) were inoculated via an intracranial route, and survival was monitored.

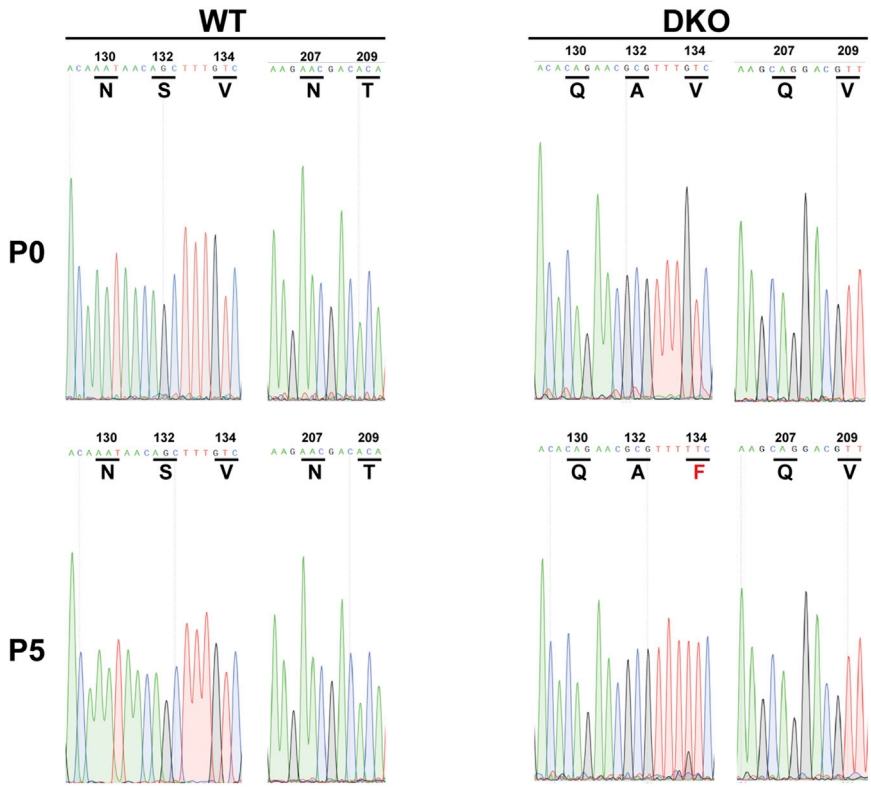

Figure S4. Sequencing Traces of NS1 Gene of Parental WT and ZIKV-NS1-LAV Viruses, Related to Figures 2 and 3

Sequence tracings of relevant NS1 gene regions (amino acids 129–134, left; 206–209, right) for the parental WT and ZIKV-NS1-LAV (DKO) viruses at initial generation from an infectious cDNA clone (P0, top) or after five sequential passages in Vero cells (P5, bottom). Apart from the stability of the mutations that destroy the two N-linked glycosylations sites in NS1, ZIKV-NS1-LAV acquired a separate adaptive mutation (V134F) during passage (indicated in red), which enhanced growth in Vero cells.

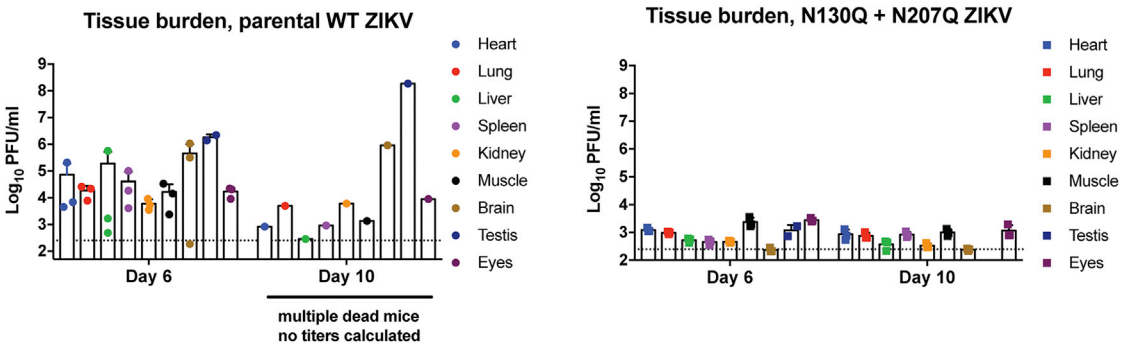

Figure S5. Viral Burden in Different Organs of Parental and ZIKV-NS1-LAV Infected A129 Immunocompromised Mice, Related to Figure 2

Viral burden measurements in indicated tissues at days 6 and 10 after infection with parental (n = 3) and ZIKV-NS1-LAV (n = 3). Dotted line indicates limit of detection of assay.

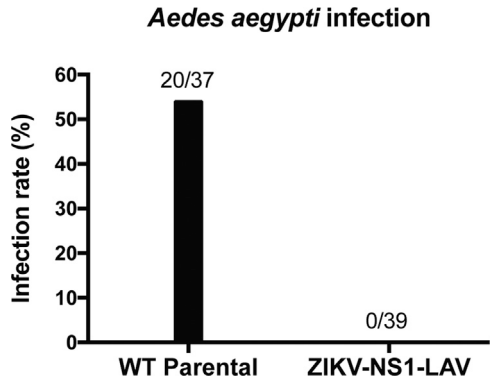

Figure S6. Mosquito Infectivity Assay, Related to Figure 2

Aedes aegypti were fed with artificial blood-meals spiked with 10^6 FFU/ml of parental WT or ZIKV-NS1-LAV. Each engorged mosquito was homogenized on day 7 post-feeding and tested for viral infection using an immunofluorescence assay on Vero cells. The total number of engorged mosquitoes and infected mosquitos are indicated above the bar graph.

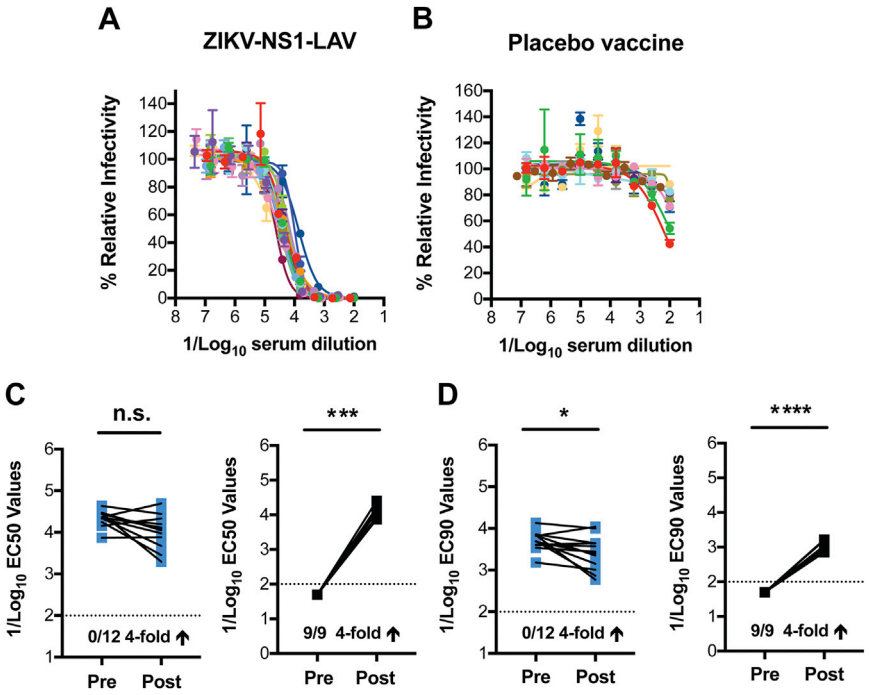

Figure S7. Neutralizing Activity of Serum from ZIKV-NS1-LAV Vaccinated C57BL/6 Female Mice, Related to Figure 3

(A and B) Eight-week-old female C57BL/6 mice in each group were immunized with 10^5 PFU of ZIKV-NS1-LAV (Group 1, (A), n = 18) or placebo (Group 2, (B), n = 11). Serum was collected at day 28 post initial vaccination and analyzed for ZIKV neutralization activity by RVP assay. Each line represents the neutralization curve from an individual mouse.

(C and D) Anamnestic neutralizing antibody response. Paired sera were collected from vaccinated animals (ZIKV-NS1-LAV or placebo) before (Pre) or 7 days after (Post) ZIKV challenge and analyzed for neutralizing activity (only pregnant animals shown). EC50 (C) and EC90 (D) values were analyzed for differences by a Wilcoxon matched paired sign-rank test (n.s., not significant; *$p < 0.05$; **$p < 0.01$). Indicated at the bottom of each graph is the number of animals showing a 4-fold increase in neutralization titer at 7 days after ZIKV challenge.